

Leonardo Dias Pereira

**Minimizing Drill String Torsional
Vibration Using Surface Active
Control**

DISSERTAÇÃO DE MESTRADO

DEPARTAMENTO DE ENGENHARIA MECÂNICA
Programa de Pós-graduação em Engenharia
Mecânica

Rio de Janeiro
April de 2017



Leonardo Dias Pereira

**Minimizing Drill String Torsional Vibration
Using Surface Active Control**

Dissertação de Mestrado

Dissertation presented to the Programa de Pós-Graduação em Engenharia Mecânica of PUC-Rio in partial fulfillment of the requirements for the degree of Mestre em Engenharia Mecânica.

Advisor: Prof. Hans Ingo Weber

Rio de Janeiro
April de 2017



Leonardo Dias Pereira

Minimizing Drill String Torsional Vibration Using Surface Active Control

Dissertation presented to the Programa de Pós-Graduação em Engenharia Mecânica of PUC-Rio in partial fulfillment of the requirements for the degree of Mestre em Engenharia Mecânica. Approved by the undersigned Examination Committee.

Prof. Hans Ingo Weber

Advisor

Departamento de Engenharia Mecânica – PUC-Rio

Prof. Rubens Sampaio Filho

Departamento de Engenharia Mecânica – PUC-Rio

Profa. Roberta de Queiroz Lima

Departamento de Engenharia Mecânica – PUC-Rio

Dr. Romulo R. Aguiar

Schlumberger Serviços de Petróleo – SLB

Prof. Marcio da Silveira Carvalho

Vice Dean of Graduate Studies

Centro Técnico Científico – PUC-Rio

Rio de Janeiro, April 25th, 2017

All rights reserved.

Leonardo Dias Pereira

The author graduated in Mechanical Engineering at Universidade Federal do Pará (UFPA) at Belém, in 2011 and completed a year of academic exchange in Mechanical and Energy Engineering at the *Istitut National Polytechnique de Grenoble* (Grenoble INP - Ense³), France, in 2009. In 2013, he started to work as Drilling and Completion Consultant at Halliburton where he stayed for four years . There, he developed a remarkable experience working and communicating with multi-disciplinary and international/multi-cultural teams achieved by the Halliburton Advanced Fast Track Program in Houston, TX, in 2014. In 2015, he won the Strive for Excellence award as the best Drilling and Completion project at Halliburton, using the relevant business acumen to implement Wellhead Movement analysis for the Petrobras casing and tubing design. In March 2016, the author started his master research in the Laboratory of Dynamic and Vibration at the Departamento de Engenharia Mecânica at PUC-Rio under the supervision of Hans Ingo Weber. The result of this research are presented in this dissertation and focus on applying control of stick-slip vibrations in drilling system.

Bibliographic data

<p>Pereira, Leonardo Dias</p> <p>Minimizing Drill String Torsional Vibration Using Surface Active Control / Leonardo Dias Pereira ; advisor: Hans Ingo Weber. – 2017.</p> <p>v., 92 f.: il. ; 29.7 cm</p> <p>Dissertação (mestrado) – Pontifícia Universidade Católica do Rio de Janeiro, Departamento de Engenharia Mecânica.</p> <p>par Inclui referências bibliográfias.</p> <p>1. Engenharia Mecânica – Teses. 2. perfuração de poços de petróleo. 3. controle de vibração. 4. coluna de perfuração. 5. stick-slip. 6. vibração torsional. I. Weber, Hans Ingo. II. Pontifícia Universidade Católica do Rio de Janeiro. Departamento de Engenharia Mecânica. III. Título.</p>

CDD: 621

To my parents, brothers and to my wife Jahnne Brandão for all the support
during this period.

Acknowledgments

The author would like to acknowledge the Department of Mechanical Engineering of PUC-Rio for the partnership that generating the support for this research. Special acknowledgments to the Laboratory of Dynamics and Vibrations for permission to work and developed the study using its resources and dependencies and specially to Wagner Epifânio for his strong support over these years. The author would like to recognize Bruno Cayres, Fernanda Ohashi and Abel Arieta for their contribution during the development of the technical and conceptual part of this dissertation. Finally, the author also would like to thank Prof. Hans Weber for his careful review of the manuscript and great contribution and motivation to finalize this study.

Abstract

Pereira, Leonardo Dias; Weber, Hans Ingo (Advisor). **Minimizing Drill String Torsional Vibration Using Surface Active Control**. Rio de Janeiro, 2017. 92p. Dissertação de Mestrado - Departamento de Engenharia Mecânica, Pontifícia Universidade Católica do Rio de Janeiro.

Part of the process of exploration and development of an oil field consists of the drilling operations for oil and gas wells. Particularly for deep water and ultra deep water wells, the operation requires the control of a very flexible structure which is subjected to complex boundary conditions such as the nonlinear interactions between drill bit and rock formation and between the drill-string and borehole wall. Concerning this complexity the stick-slip phenomenon is a major component, related to the torsional vibration and it can excite both axial and lateral vibrations. That may cause premature failure of drill-string components. So, the reduction and avoidance of stick-slip oscillations are very valuable items in terms of savings and exploration time. With these intentions, this study has the main goal of confronting the torsional vibration problem using a real-time robust control strategy. The approach is obtained following some steps such as: Open-loop analysis of the drilling system considering a top-drive actuator and the drill-string system; Design of a novel controller using different angular velocity setpoints in a closed-loop system; Control of the torsional vibration considering the nonlinearity due to friction interaction in the wall and in the donwhole system; valuate a non-stop control system while drilling; Verification by numerical simulations. In this presentation the theoretical basis behind the drilling system will be given, as well examples of numerical results providing a stable and satisfactory controlled drilling operation.

Keywords

oilwell drilling; vibration control; drill string ; stick-slip; torsional vibration.

Resumo

Pereira, Leonardo Dias; Weber, Hans Ingo. **Minimização da Vibração Torcional em uma Coluna de Perfuração Utilizando Controle com Acionamento na Superfície**. Rio de Janeiro, 2017. 92p. Dissertação de Mestrado - Departamento de Engenharia Mecânica, Pontifícia Universidade Católica do Rio de Janeiro.

Parte do processo de exploração e desenvolvimento de um campo de petróleo consiste nas operações de perfuração de poços de petróleo e gás. Particularmente para poços de águas profundas e ultra-profundas, a operação requer o controle de uma estrutura muito flexível que é sujeita a condições de contorno complexas, tais como as interações não-lineares entre broca e formação rochosa ou entre a broca e a parede de poço. Quanto a esta complexidade, o fenômeno stick-slip é um componente primordial relacionado à vibração torsional. Este pode excitar vibrações tanto axiais quanto laterais. Isso pode causar falha prematura de componentes de corda de perfuração. Assim, a redução e eliminação de oscilações do tipo stick-phase são itens muito valiosos em termos de economia financeira e de tempo de exploração. Com este propósito, este estudo tem como principal objetivo confrontar o problema de vibração torsional simulando uma estratégia de controle robusto em tempo real. A abordagem é obtida seguindo alguns passos, tais como: análise em malha aberta do sistema de perfuração considerando um atuador top drive e o sistema de coluna de perfuração; concepção de um novo controlador que utiliza diferentes velocidades angulares de referência num sistema de controle de malha fechada; controle da vibração torsional considerando a não-linearidade devida à interação de atrito na parede do poço e no fundo do poço; avaliar por meio de simulações sistemas de controle ininterruptos durante a perfuração; validação dos modelos por meio de simulações numéricas. Esta dissertação apresenta a base teórica por trás do sistema de perfuração, bem como exemplos de resultados numéricos que proporcionam uma operação de perfuração controlada estável e satisfatória.

Palavras-chave

perfuração de poços de petróleo; controle de vibração; coluna de perfuração; stick-slip; vibração torsional.

Table of contents

1	General introduction	18
1.1	Oilwell drilling overview	18
1.2	Motivation and objectives	23
1.3	Methodology	24
1.4	Outline of the dissertation	25
2	Literature review and preliminary concepts	27
2.1	Introduction	27
2.2	Literature review on active drill string control techniques	28
2.2.1	Classical control strategy	28
2.2.2	Robust control strategy	30
2.3	Preliminary concepts	33
2.3.1	Basic control definitions	33
2.3.1.1	Dynamical system	33
2.3.2	Open-loop and closed-loop systems	35
2.3.2.1	Open-loop system	35
2.3.2.2	Closed-loop system	36
2.3.3	Automatic control systems	38
2.3.4	Proportional, integral and derivative actions and controllers	39
2.3.4.1	Proportional action	39
2.3.4.2	Integral action	39
2.3.4.3	Derivative action	39
2.3.4.4	Proportional and integral controller (PI)	40
2.3.4.5	Proportional, integral and derivative controller (PID)	40
2.3.5	Model predictive control (MPC)	41
3	Mathematical modeling of the dynamical drilling system	45
3.1	Introduction	45
3.2	Dynamic modeling	45
3.2.1	Modeling approach: two degrees of freedom	45
3.2.1.1	Lower system: torsional pendulum	46
3.2.1.2	Upper system: DC motor	49
3.2.2	State-space equation of the electromechanical system	50
3.2.3	Friction torque modeling	50
4	Control design: open-loop and closed-loop approaches	53
4.1	Introduction	53
4.2	The open-loop analysis	53
4.2.1	Mathematical simplifications for the open-loop analysis	56
4.3	Closing the loop	57
4.3.1	Mathematical simplifications for the closed-loop control	58
4.4	Controlling nonlinear disturbance in drilling system	58
4.5	Stick-slip severity (SSS)	58

5	Analysis of the results	60
5.1	Introduction	60
5.2	Simulation results of the open-loop systems	60
5.3	Simulation results of the closed-loop system without disturbance	65
5.4	Simulation results of the closed-loop system with disturbance	67
5.4.1	Proportional and integral controller (PI)	67
5.4.2	Proportional, integral and derivative controller (PID)	72
5.4.3	Model predictive controller (MPC)	76
5.4.4	MPC and PID controllers (MPC+PID)	80
6	General conclusions and future works	83
6.1	Conclusions	83
6.2	Recommendations for future research	85
	Bibliography	92

List of figures

1.1	Components of an oilwell drilling system. (Source: State of California, 2005)	20
1.2	Types of drill string vibrations. Source: López, [1].	21
1.3	Simulated Stick-Slip phenomenon. (Ω_1 – drill bit / Ω_2 – top drive).	22
2.1	Block diagram representing a general System.	33
2.2	Block diagrams of open-loop systems.	36
	2.2(a)Open-loop system with feedforward control	36
	2.2(b)Open-loop system without feedforward control	36
2.3	General block diagrams of a closed-loop system.	37
2.4	Major steps in model-based control design. (Adapted from Seborg (2004) [2]).	42
2.5	Block diagram for MPC. (Adapted from Seborg (2004) [2]).	43
2.6	Basic concept for MPC. (Adapted from Seborg (2004) [2]).	44
3.1	Schematic of modern drilling system.	46
3.2	A drill string system modeled as a torsional pendulum.	47
3.3	Electrical equivalent circuit of armature.	49
3.4	Static + Coulomb + Negative damping friction model.	52
4.1	Block diagram of the closed-loop drilling system.	54
4.2	Process of opening the loop of the drilling system.	55
4.3	Block diagram of the open-loop DC motor.	55
4.4	Block diagram of the open-loop drill string.	55
4.5	Block diagram of the closed-loop drilling system without disturbance.	57
4.6	Stick-slip severity curves for the four control strategies.	59
5.1	The iterative open-loop flowchart used in the analysis.	61
5.2	Angular velocity and torque responses	63
	5.2(a)($2kN \cdot m - 10kN \cdot m$)	63
	5.2(b)($12kN \cdot m - 20kN \cdot m$)	63
	5.2(c)($2kN \cdot m - 10kN \cdot m$)	63
	5.2(d)($12kN \cdot m - 20kN \cdot m$)	63
5.3	Stick-slip severity curve for open-loop system without control.	65
	5.3(a) 3D map	65
	5.3(b) 2D map	65
5.4	Angular velocity responses for PID controller.	65
	5.4(a) ($2kN \cdot m - 10kN \cdot m$)	65
	5.4(b) ($12kN \cdot m - 20kN \cdot m$)	65
5.5	Calculated SSS and Bifurcation diagrams for PI controller.	68
	5.5(a) 3D map	68
	5.5(b) 2D map	68
	5.5(c) $\Omega_{ref} = 79,36$ rpm	68
	5.5(d) $WOB = 160$ kN	68
5.6	Closed-loop simulation of a top drive system (Case 1).	69

5.7	Closed-loop simulation of a top drive system (Case 2).	70
5.8	Closed-loop simulation of a top drive system (Case 3).	70
5.9	Closed-loop simulation of a top drive system (Case 4).	71
5.10	Closed-loop simulation of a top drive system (Case 5).	71
5.11	Calculated SSS and Bifurcation diagrams for PID controller.	72
	5.11(a)3D map	72
	5.11(b)2D map	72
	5.11(c) $\Omega_{ref} = 79,36$ rpm	72
	5.11(d) $WOB = 160$ kN	72
5.12	Nonlinear angular velocity responses for PID controller.	73
5.13	Nonlinear response of a PID Closed-loop system.	74
5.14	Calculated SSS and Bifurcation diagrams for MPC controller.	76
	5.14(a)3D map	76
	5.14(b)2D map	76
	5.14(c) $\Omega_{ref} = 79,36$ rpm	76
	5.14(d) $WOB = 160$ kN	76
5.15	Nonlinear angular velocity responses for MPC.	78
5.16	Nonlinear response of a MPC Closed-loop system.	78
5.17		80
	5.17(a)3D map	80
	5.17(b)2D map	80
	5.17(c) $\Omega_{ref} = 79,36$ rpm	80
	5.17(d) $WOB = 100$ kN	80
5.18	Nonlinear angular velocity responses for MPC+PID controller.	81
5.19	Nonlinear response of a MPC+PID Closed-loop system.	82

List of tables

3.1	Friction factors values used in the friction modeling.	52
5.1	Simulation parameters values.	62
5.2	Drill string and DC Motor open-loop results.	63
5.3	Attributes of the drill string step responses.	64
5.4	Attributes of the DC motor step responses.	64
5.5	PID controller parameters tuned.	65
5.6	Attributes of the drill string step responses.	66
5.7	Drill-string and Closed-loop simulation performance.	66
5.8	PI controller parameters tuned.	67
5.9	Cases of transition functions.	69
5.10	Attributes of the drill string step responses with PID.	74
5.11	Drill string with PID simulation performance.	75
5.12	Attributes of the drill string step responses with MPC.	77
5.13	Drill string with MPC simulation performance.	79
5.14	Attributes of the drill string step responses with MPC+PID.	81
5.15	Drill string with MPC + PID simulation performance.	82

Nomenclature

List of abbreviations

Peak	first maximum value reached by y
ADS	active damping system
BHA	bottom hole assembly
D-OSKIL	drilling oscillation killer
DC	drill collars
DC motor	direct current motor
DOF	degrees of freedom
DRPM	downhole RPM
DTF	data transmission frequencies
DWOB	downhole WOB
FEM	finite element methods
GA	genetic algorithms
GUI	graphical user interface
HWDP	heavy weight drill pipe
KSEPL	Koninklijke/Shell Exploratie en Productie Laboratorium
MPC	model predictive controller
N/A	Not Applied
NMPC	nonlinear model predictive controller
OPEC	Organization of the Petroleum Exporting Countries
OSKIL	oscillation killer
PI	proportional and integral controller
PID	proportional, integral and derivative controller
ROP	rate of penetration
RPM	rotations per minute
SRPM	surface RPM
SSS	stick-slip severity
STOR	surface torque

STRS	soft torque rotary system
TFC	torque feedback control
TOB	torque on bit
WOB	weight on bit

List of symbols

%OS	Overshoot – percentage overshoot (relative to y_{final})
$\hat{y}(k_t)$	predicted outputs
μ	constant friction coefficient
ν	Poisson ratio
Ω_1^{max}	maximum angular velocity of the drill bit
Ω_1^{min}	minimum angular velocity of the drill bit
Ω_1	angular velocities measured at the downhole (DRPM)
Ω_2	angular velocities measured at the surface (SRPM)
Ω_{dyn}	final speed of the sticking regime
Ω_{ref}	reference angular velocity
ρ_{bha}	BHA mass density
ρ_{dp}	drill string mass density
τ_p	Peak time – time at which this peak is reached
τ_r	Rise time – time to first reach the steady-state value
τ_s	Settling time – time to reach and remain above the steady-state value
φ_1	angular displacements of the BHA
φ_2	angular displacements of the top drive
C_1	equivalent viscous damping coefficient of downhole
C_2	equivalent viscous damping coefficients of surface
Dr	damping factor of the mud
E	Young's modulus
e	control error ($e = [r(t) - y_m(t)]$)
$E(t)$	control error ($E(t) = [\Omega_{ref} - \Omega_2]$)
e_c	stability error criterion

I	armature current
I_{bha}	area moment of inertia for the BHA
I_{dp}	area moment of inertia for the drill pipe
ID_{bha}	BHA inner diameter
ID_{dp}	drill string inner diameter
J_1	equivalent mass moment of inertia of the BHA
J_2	equivalent mass moment of inertia of the surface
k	equivalent torsional stiffness coefficient of the drill pipe
k_t	actual sampling instant
k_d	derivative gain, ($k_d = k_p \dot{T}_d$)
k_e	electromotive force constant
k_i	integral gain, ($k_i = \frac{k_p}{T_i}$)
k_p	proportional gain
k_t	motor torque constant
L	electrical inductance
L_{bha}	BHA length
L_{dp}	drill string length
OD_{bha}	BHA outer diameter
OD_{dp}	drill string outer diameter
P_{f-c}	Coulomb factor
P_{f-nd}	negative damping approximation
P_{f-neg}	“negative” friction factor when the angular velocity reaches negative values
P_{f-s}	static factor
$P_f(\Omega_1)$	velocity-dependent proportional friction factor
R	electrical resistance
r	manipulated variable
S_{input}	input signal of the controller
SSS	stick-slip severity - instability criterion
T_m	torque input signal of the drilling system

T_1	nonlinear function representing the downhole TOB
T_d	derivative time constant
T_i	integral time constant
Tol	speed tolerance
$u(k_t)$	actual input
u_c	control signal
U_m	voltage input signal of the actuator / motor input voltage
V_{emf}	back-electromotive force (back-emf)
V_{input}	voltage input signal of the actuator
y	output angular velocity of the drill string
y_m	controlled variable
$\{\mathbf{A}_1\}$	set parameters coefficient matrix
$\{\mathbf{A}_2\}$	input parameter vector
$\{\mathbf{A}_3\}$	output parameter matrix
$\{\mathbf{C}\}$	matrix of damping
$\{\mathbf{J}\}$	matrix of inertia
$\{\mathbf{K}\}$	matrix of stiffness
\mathbf{q}'	first derivative of the state vector
\mathbf{T}	torque disturbance vector
\mathbf{y}	output vector
u	scalar control law
\mathbf{q}	state vector

Excellence is an art won by training and habituation. We do not act rightly because we have virtue or excellence, but rather we have those because we have acted rightly. We are what we repeatedly do. Excellence, then, is not an act but a habit.

Aristotle, *The Story of Philosophy*.

1

General introduction

1.1

Oilwell drilling overview

Over the last 20 years, the world has watched the volatility on global supply/demand mechanism and on the oil and gas market expectations. Demand for oil is related to economic activity, so the higher the economic activity the higher oil demand. As to the seasonal aspects, it spikes for example during winter time in the northern hemisphere. On the other hand, supply is determined by weather (can affect production) and by geopolitical issues (can affect the crude oil price) [3].

For example, in the mid-2000s, global demand for crude oil was rising. This situation resulted in a tight market and steep price increases [4]. However, global oil prices have fallen sharply over the past two years, resulting in one of the most dramatic declines in the price of oil in recent history. The oil prices have collapsed from around \$114 in June 2014 to \$28 in February 2016 [3].

To be more specific, between December 2010 and July 2014, oil barrel prices were quoted, on average, above 100 dollars [3]. Then, still in 2014, the Organization of the Petroleum Exporting Countries (OPEC) - responsible for supplying 40% of the world's crude oil - increased its oil production by the largest volume in almost three years. Meanwhile, the US continued to increase its shale production. As a result, the global production increased faster than its demand, creating a long market [4].

To make the shale oil exploration economically viable, the United States has invested in several resources, such as an advanced oil exploration and production infrastructure. The unconventional technologies used for shale extraction could be used to boost the production of existing conventional oil fields globally [3].

The use of increasingly sophisticated drilling techniques and huge improvements in cost efficiencies has not only reduced the costs associated with the production of shale oil, but it has also made the extraction resemble a manufacturing process. In other words, the quantity produced can be altered in response to price changes with relatively ease. This is not the case for conven-

tional oil extraction which requires large capital expenditure and lead times.

The drilling time for shale oil continues to become increasingly more efficient. Two years ago, it took six weeks to drill a single well. Today, it takes approximately two weeks. Cost-saving technologies include more efficient exploration methods, onsite automation systems, and intelligent production monitoring software. Beyond cheaper hardware, the next saving opportunity lies in advances including more automation: intelligent control systems requiring less physical workforce, less downtime and improving yields of existing wells. It is worth mentioning that due to the current advances in shale oil production it now takes only 20 days and \$10 million to drill for shale while it takes \$10 billion and five to ten years to launch a deep water oil project [3].

The example of shale recovery history demonstrates that the actual organizational model of oil and gas industry is no longer sustainable with oil prices below \$50 a barrel. Christopher *et al.* (2016) [5] describes what they call the “potentially game-changing disruptions that may lead oil and gas companies to rethink their operating models fundamentally”. Here, two of the main reasons are pointed to elucidate what this study intends to emphasize:

1. “A world of resource abundance is leading to sustained lower oil prices and a focus on cost, efficiency, and speed. Talent is no longer scarce, exploration capability is less of a differentiator, mega-projects are not the only way to grow and market opportunities may only be economical for the earliest movers in a basin. Meanwhile, conventional, deep water, unconventional, and renewable assets each require a distinct operating model that cannot be delivered optimally from a single corporate center”.
2. “Profound technological advances are disrupting old ways of working and enabling steep changes in productivity. Jobs, including knowledge work, are being replaced by automation on a large scale, and those that remain require increased human-machine interaction. Data generation continues to grow exponentially, as every physical piece of equipment wants to connect with the cloud. This explosion of data - combined with advanced analytic and machine learning to harness it -creates opportunities to fundamentally re-imagine how and where work gets done”.

Then, to address these challenges, this study focuses its efforts on the conventional drilling operations. These are an important part of a process of exploration and development of oilfields. In this context, the rotary drilling system is considered the most used drilling technique in the petroleum industry. This process involves rock failure by a rotating **drill bit**. To rotate this drill bit from the top-end position (surface), the drilling rig’s power source is used

to turn a **rotary table**. A mechanism, composed of the **master bushing** and **kelly**, is used to transmit the rotation from the rotary table to the drill string.

An electric or hydraulic **top drive** unit is used as an alternative to the conventional arrangement on modern rigs. In this situation, the rotational energy is transmitted directly from the rig's power source to the drill string.

The subsurface component through which torque is transmitted from the surface to the bottom of the drilling system (downhole) is the drill string. The drill string consists of connected lengths of **drill pipes**, the **bottom hole assembly (BHA)**, and the **drill bit**. The BHA is the portion of the drill string between the drill pipe and the drill bit. It is made up, primarily, of **drill collars (DC)** and **heavy weight drill pipe (HWDP)**. These components, shown in the Fig.1.1, are responsible for the open hole creation.

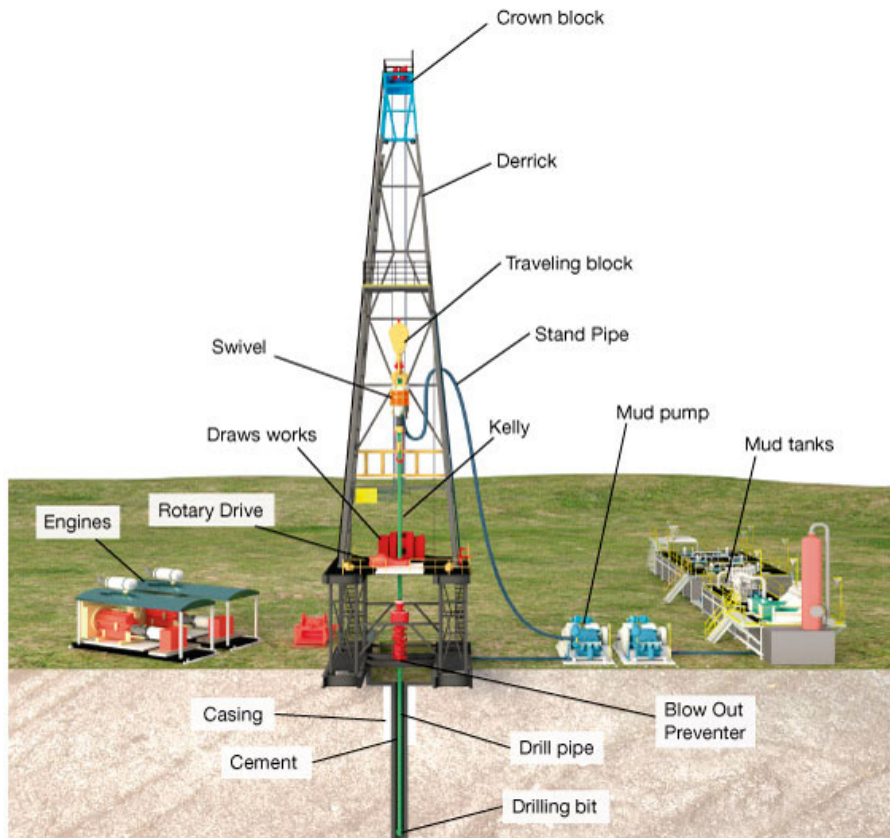


Figure 1.1: Components of an oilwell drilling system. (Source: State of California, 2005)

The operational sequences to drill a hole section are based on standard drilling procedures. Of course, they may change over the years. But they are always monitored by a driller who can adjust critical drilling parameters from a control device in the rig floor. For example, the driller may set up the top

drive to rotate at a constant revolution (**rotations per minute - RPM**). Also, the driller may adjust the amount of **hook load** applied [that reflects on the **weight on bit (WOB)**]. Other parameters, such as **torque on bit (TOB)** and the **rate of penetration (ROP)**, also allow the driller to be informed of any potential problem [6, 7, 8].

Particularly for deep water and ultra-deep water wells, the operation described above requires the control of a very flexible structure (the drill string length may be up to 5 km for ultra deep water whereas its diameter is typically less than 150 mm) which is subjected to complex boundary conditions. The complexity may be due to the nonlinearity between drill bit and rock formation and between the drill string and borehole wall. Hence, dynamic drilling systems can present complex vibrational states and there is a strong need to understand them in order to better control the drilling operation and improve the ROP.

Previous studies have identified three types of vibrations that may occur during drilling operations, as illustrated in Fig. 1.2. They are classified as [9, 10]:

Torsional - large amplitude fluctuations of the angular velocity due to large torsional flexibility of the drilling assembly.

Axial - motion of drilling components along its own longitudinal axis.

Lateral - whirl motion due to the out-of-balance of the drill string.

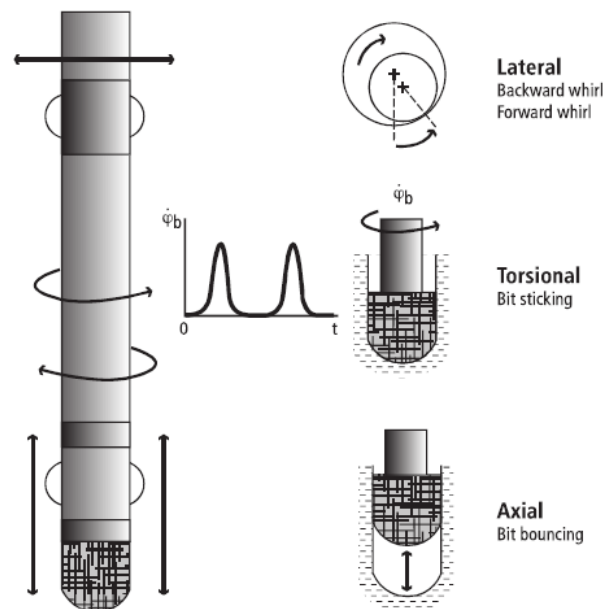


Figure 1.2: Types of drill string vibrations. Source: López, [1].

According to some authors [10, 11] the stick-slip behavior of the drill string represents one of the most severe case (in terms of oscillation amplitudes

and drill string life cycle reduction) of torsional vibration and instability on the drilling system dynamics. More specifically, the torque applied at the bit is governed by the bit-rock interaction law [12, 13] and depends on the angular velocity at the rock-bit interface. Basically, the nonlinearity in the relationship between the pair {WOB, RPM} defines the behavior of the system: the stick-slip is observed at low RPM or high WOB; and it does not observed at high RPM and low WOB [13].

In recent years, several controlled systems were designed to maintain an angular velocity nearly a constant value at the surface. But this situation does not assure the same condition at the drill bit. That happens because the stick-slip phenomenon may drive the system to a highly oscillating angular velocity at the bottom. In extreme cases, this oscillation may lead to a complete arrest of the drill bit (stick phase), while the drill string is still being torqued-up. Then, the drill bit rotation is released (slip phase) and it rotates at a much higher angular velocity than the desired (up to 5 times the adjusted velocity). Fig. 1.3 illustrates the stick-slip behavior when the $WOB = 120$ kN and $\Omega_{ref} = 60$ rpm.

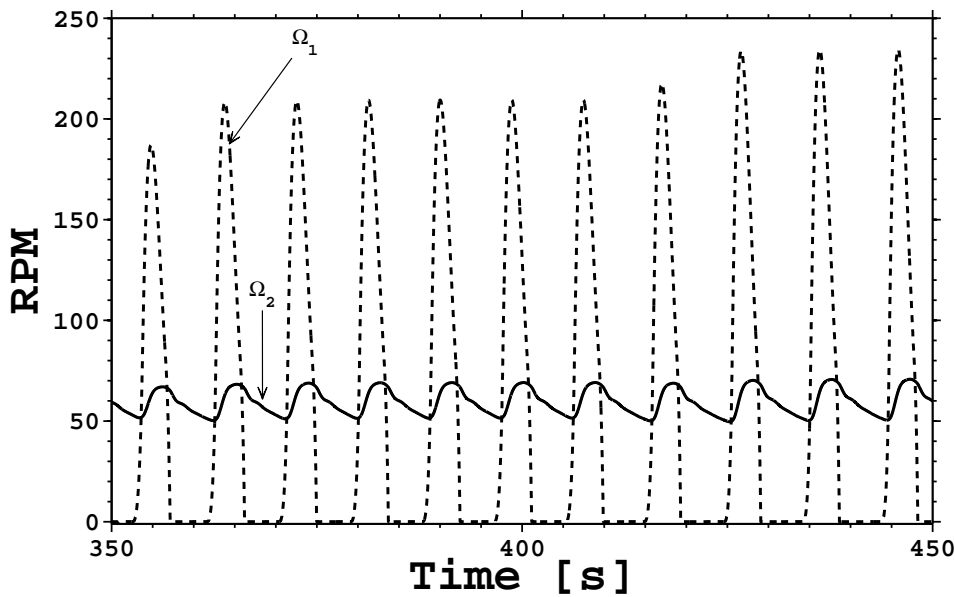


Figure 1.3: Simulated Stick-Slip phenomenon. (Ω_1 — drill bit / Ω_2 — top drive).

The stick-slip can be defined as a periodic and stable oscillation of the angular velocity for several drilling conditions [14]. This oscillation uses the energy accumulated to self-excite itself and, generally, disappears as the desired RPM is increased and/or the WOB is reduced under certain drilling conditions. However, at higher angular velocities, some other complex phenomena appear, such as lateral vibrations (backward and forward whirling), impacts of drill string on borehole wall, and parametric instabilities.

Therefore, to improve the drilling conditions for relatively low angular velocities, several studies on drill string dynamics, with focus on dynamical models and control design, exist in the literature. Some of them will be presented in section 2.2.

1.2

Motivation and objectives

Drilling operation represents an expensive phase of the oil and gas prospecting. They represent approximately 40% of all exploration and production (E&P) costs [15]. Due to its high costs, drilling has become the main challenge of oil and gas exploration. The drill string vibration is responsible for a large percentage of failures due to different excitations sources, such as non-linear bit-rock interactions, mass imbalance, misalignment, mud motor, and friction between the drill pipe and borehole wall.

Studies focusing on torsional vibrations of drill chords have shown that stick-slip behavior occurs 50% of the time in drilling processes and can excite both axial and lateral vibrations. These vibrations can cause premature equipment failure [16]. Thus, it is clear that the reduction and avoidance of torsional vibrations (stick phase) are very valuable in terms of savings and operating time.

Since the vibration problems were detected and identified in the drilling process, several approaches have been suggested, both in industry and literature, to model and control these vibrations. Some of the approaches were driven to the surface system. Most of them dealt with the torsional behavior and the suppression of the stick-phase in the stick-slip oscillations [17]. Moreover, the nonlinearity and the system parameter incertitude have been modeled into the control design process.

Another important consideration to be taken in the system is the time delay in measurements. They might cause problems while running real-time controls [18].

The scope of this study is to minimize the torsional vibration problem of the drill bit using existing control strategies. In addition, evaluation and confronting their performances will be considered. The specific objectives deal with:

- Open-loop analysis of the drilling system considering a saturated and a non-saturated top drive actuator.
- Application of existing control strategies using different torque/velocity input in a closed-loop system.

- Control of the torsional vibration considering the nonlinearity due to friction interaction with the wall and in the donwhole system.
- Evaluate a non-stop control system while drilling.
- Improvement on a developed experimental reduced setup to future verification and validation of the models.

1.3

Methodology

The methodology required to evaluate the performance of the control drilling system are based on five steps:

1. The modeling of the mechanical and mathematical representation of the drilling system is developed.
2. An open-loop analysis is performed to a simplified model using a linear motor and a two degrees-of-freedom (DOF) system. In this system a friction model with parameters that generate torsional vibrations at the bit is proposed, i.e. a settled relation involving WOB, surface torque (STOR), TOB, and desired input RPM (Ω_{ref}).
3. The state-space environment is designed to reconstruct the states variables needed to control the bit vibration.
4. The closed-loop analysis starts assuming a set of parameters for different controllers.
5. Two situations are analyzed concerning the control strategies:
 - (a) Only surface parameters such as STOR, surface RPM (SRPM), and WOB are known.
 - (b) The surface and the downhole measurements (such as TOB, downhole RPM [DRPM], and downhole WOB [DWOB]) are known.

Another concern is the way to collect the measurements from the surface or from the downhole to be sent to a control device. In fact, there are many different data transmission frequencies (DTF) for both cases. The DTF can be estimated from the type of transmission used in field, i.e. telemetry signals or wired drill pipe [19]. Thus, for both surface and downhole cases, a determination must be made as to whether or not it is possible to control the drilling system for a specific number of DTFs (chosen according to the existing DFTs).

Finally, the methodology elaborated here can be continuously used for systems with varying number of DOFs, chosen according to increasing modeling complexity of the drill string components.

One of the most important results of this study is a program performed in *Simulink* environment to achieve the explained methodology. The *Simulink* software was used because it provides a graphical user interface (GUI) for building models as block diagrams. Hence, the interface can build models, simulate and analyze the dynamical drilling system. Then, the proposed model simulations assume the drill string as a torsional pendulum composed of a generic number of DOF. In addition, the user can set the number of DOF.

For result analysis of the proposed drilling system, in *Simulink* environment, it can plot chosen inputs and outputs parameters. So, it is possible to predict the dynamic behavior of the model in surface and downhole.

Another important achievement of this study is that it uses the *Simulink* to compare different control strategies used to optimize drilling performance. This comparison aims to determine the most effective control strategy among a variety of alternatives. For this propose an optimization criterion and a robust stability criterion of the system are combined using the *Simulink* toolbox.

Initially, there are four control strategies used in this comparison:

- Proportional and Integral Controller (PI)
- Proportional, Integral and Derivative Controller (PID)
- Model Predictive Controller (MPC)
- Proportional, Integral and Derivative and Model Predictive Controller (PID + MPC).

In the end, the study will discuss about an experimental test rig constructed in the laboratory for future validation and a test of a reduced real-time model. This system will be further discussed in the section of suggestions for future studies.

1.4

Outline of the dissertation

The dissertation is based on work performed in the Pontifical Catholic University of Rio de Janeiro (PUC- Rio) for a scientific and technological graduate program to obtain the Master degree. The dissertation is organized as following. First, in Chapter 1 the general introduction about the oil and gas industry and the proposed problem are presented. To understand what was done in the past the Chapter 2 presented a literature review in control torsional vibration and ends the Chapter with the preliminary concepts of the control strategies used in this study. Then, Chapter 3 presented the Mathematical modeling to describe the problem and further simplifications of the proposed model. Chapter 4 presented the methodology used to desing the control strategies adopted. The simulation results and a preliminary analisis

are presented in Chapter 5. Finally, the study conclusions and future works are discussed in Chapter 6.

2

Literature review and preliminary concepts

2.1

Introduction

The overview about the oilwell industry presented in the last chapter showed that stick-slip vibration is one of the primary causes of drill string component failures. For that reason, several studies and actions have been taken to optimize the drilling operation and/or avoid drill string vibration. Nevertheless, there is still a giant field to be developed about this concern that also motivated the current study.

Over the past 70 years, there were hundred of references about the vibration on drilling systems. Many of them were taken to develop analysis methodologies, evaluation technologies and control methods for the drill string vibrations. Moreover, according to the control theory and control engineering knowledge, these control methods can be divided into passive control, active control, and semi-active control [20]. However, only in the last 30 years a significant variety of control actions have been developed to suppress the stick-slip phenomenon. There are so many options that it is impossible to determine which approach is the best, as they all have benefits for some drilling conditions [21].

In this chapter, approaches for stick-slip vibration suppression are focused on, and the developments in the theoretical background are conducted. First, the approaches for stick-slip vibration active control are reviewed by grouping the literature references under two different categories: classical and robust control strategies. Then, the theoretical basis of control, applied to drilling systems, is briefly reviewed. Furthermore, additional reviews about drill string vibration can be found on the references [21, 20].

2.2

Literature review on active drill string control techniques

2.2.1

Classical control strategy

Halsey *et al.* [16] were the very first to model an active control strategy to eliminate, or at least reduce, self-excited torsional drill string vibrations occurring due to the stick-slip phenomena. The Torque Feedback Control (TFC) developed by Halsey *et al.* had the goal to correct the demanded speed according to the torque signal measured at the rotary table. They verified their results by field experimentation on a full-scale research drilling rig and used accelerometers in the downhole components. They concluded that the conventional speed controller made the top drive very insensitive to torque load variations. They also concluded that such a control system leads to smoother rotation of the bit which can lead to a reduction in axial and lateral vibrations of the drill string.

In 1992, Sananikone *et al.* [8] proposed to make a comparison between the TFC, the combined motor current and acceleration feedback system, and the motor current only feedback system. Drilling field operations had been done to evaluate the performance looking at the "reflection". This coefficient is related to the vibration wave. This energy is reflected back down in the drill string. Some applications which should be added on were addressed in this study, such as a surface torque limiting system to prevent excessive winding up of the drill pipe. They concluded that the TFC described has the advantage of being simpler to install than the simple torque feedback system, reducing drill string vibrations by 90% and of not requiring "re-tuning" for different drill string lengths.

Still in 1992, a modified version of the TFC was developed and field-tested by Koninklijke/Shell Exploratie en Productie Laboratorium (KSEPL) and Deutag Drilling Inc. of Germany [22, 23]. This system was called Soft Torque Rotary System (STRS) and relied on a minor modification of the electronic speed control system on the drive system. If the current of the rotary drive motor was a measure of the torque at the surface, the current could be directly used to control the velocity of the motor, thus eliminating the need for torque measurement at the rig floor [22, 23]. The principles of the STRS are detailed by Worrall *et al.* [24] patent. Javanmardi and Gaspard [23] also commented on the successful field test performed in several top drive rigs, but they focused primarily on the Mobile Bay application. They observed that different sizes of drill strings exhibit different vibratory characteristics,

so the STRS has to be tuned for each drill pipe size used on the rig. They concluded that the STRS had significantly reduced torque fluctuations (up to 80%), torsional drill string vibrations, and the bit stick-slip motions.

Jansen & van den Steen [25] also explored the idea of the TFC based on the same principles explained in [16, 8]. In this study Jansen applied an active damping system (ADS) describing how it strongly reduced a threshold value of the angular velocity by using feedback control. They highlighted the nonlinear relation between torque and angular velocity at the bit. This relation generates the self-excited torsional drilling vibrations. They also used the electrical variables to perform the ADS such as Sananikone [8] did, but without the accelerometer at the motor shaft. However, the main contribution of this article is the ease use of the TFC and the ADS. Jansen concluded the paper discussing the applicability of such system for different types of motors, other than DC motors. This application is shown in their other study, reference [26].

The linear H_∞ control design technique proposed by Serrarens [7] aimed to suppress the stick-slip oscillations and transient behavior of the angular velocity improved over a PD control system. Serrarens was the first to apply a robust closed-loop system to treat the nonlinear friction influence. This paper concluded that the designed controller is sufficiently robust against variations in the drill string length. The paper also compared the time domain results of the H_∞ to the first-order control system STRS. It brought significant improvements to the drilling performance because the H_∞ controller suppresses limit cycles for backlash torques which are much higher than those handled by the STRS controller. These results were proven experimentally and the numerical simulations showed great resemblance with the experimental responses.

Kriesels *et al.* [15] discussed the use of some specific combined technology and methodology developed to solve drill string torsional vibration and its effects when using STRS. The control system developed by van den Steen [6] operated as a small modification of the electric motor and it suppressed torsional oscillations of the drill string. The article showed how other types of vibrations could be prevented by using vibration analysis software. It proved that applying these methods the ROP would increase and equipment damages would also decrease.

In 1999, Tucker *et al.* [27] modeled the torsional vibration of a vertical drill string driven by a controlled torque at the surface top drive and subjected to torsional friction at the bit. Tucker approached the problem of the volatility with a classical controller as PI. They explored alternative mechanisms to

disable the need for repeated retuning as the drilling characteristic varies. The paper studied the behavior of two continuous models based on axisymmetric configuration and a simplified forced torsional pendulum. In both cases the superiority of the proposed torsional rectification method over conventional control techniques had been demonstrated. Finally, the authors believed that a more robust controller (in terms of instability) could be constructed by combining existing speed controllers with torsional rectification control. That is because the combination of controllers would act on different concerns about drilling process, such as non-linear controllers and speed linear controllers.

2.2.2

Robust control strategy

To compensate the nonlinear friction effect, Abdulgalil & Siguerdidjane [14] proposed a friction compensation method using in a simple nonlinear controller for a drill string system. Therefore, the application of a nonlinear friction model, reported in the reference [14], allowed the authors to study and suggest a compensation technique for stick-slip combined with the PI controller. To confirm the proposed method efficiency some simulations were performed, demonstrating the relevance of the nonlinear friction compensation method.

In 2005, Abdulgalil & Siguerdidjane [28] proposed another robust strategy based on a nonlinear control design approach called *Backstepping* control. The backstepping technique represented a powerful and systematic strategy that recursively interlaces the choice of a Lyapunov function with the feedback control design. Afterwards, Abdulgalil & Siguerdidjane [9] presented another robust PID controller based on sliding surface function. This function worked in conjunction with an input-state control design capable to deal with a nonlinear drilling system due to uncertainties in the measured signals. The sliding mode technique is applied by choosing the bit angular velocity error as the sliding surface. Considering that, Abdulgalil & Siguerdidjane papers may be considered pioneers in this application even if Serrarens [7] methodology is used.

A different methodology to eliminate undesired limit cycles in nonlinear systems was proposed by Canudas-de-Wit *et al.* [29] in 2005. They named the Oscillation Killer (OSKIL). This strategy was applied to suppress stick-slip oscillations in the well drill string system by using the WOB as an additional control variable to extinguish limit cycles when they occur. They also created a new strategy: the Drilling Oscillation Killer (D-OSKIL) [30]. The D-OSKIL mechanism permitted elimination of the stick-slip in the drilling

system without changing the imposed angular velocity. This angular velocity is fixed by a typical speed controller.

Then, in 2006, Corchero *et al.* proposed a stability analysis of a variant of the D-OSKIL mechanism. This analysis has shown that this algorithm is globally asymptotically stable [31], thus, effectively eliminating the stick-slip oscillations. Canudas-de-Wit wrote two other papers describing this mechanism in [32, 33]. The D-OSKIL was also applied by Jijón *et al.* in 2010. They combined the control system with an unknown parameter adaptive observer that measured the angular velocity of the bit. The observer was implemented in a testbed using a mud-pulse telemetry and an acoustic data transmission over a drill string.

In 2007, Navaro-López and Cortés proposed to use a nonlinear approach to reduce and/or avoid the torsional stick-slip phenomenon. The sliding mode control is the nonlinear approach applied to the multi-DOF drilling system used to eliminate the bit sticking phenomena [34]. The drilling system consists of four kinds of elements divided in the top-rotary system, the drill pipes, the drill collars, and the bit. In their article Navaro-López and Cortés also showed robustness under parameters variations [34].

In 2009, Karkoub *et al.* proposed to use PID and lead-leg controllers combined with genetic algorithms (GA) to control the drilling system. The reason that made this technique attractive to control systems was its capability to perform with minimal knowledge of the plant under investigation [35]. The problem is converted to an optimization problem while it selects the optimum controller parameters. The authors simulated the open-loop dynamics compared to the closed-loop one. Finally, the controllers were designed using different objective functions and parameter search limits, concluding that the results were satisfactory [35].

In 2010, the slide mode control was also applied by Qi-zhi *et al.* to a conventional model describing the torsional behavior of a generic vertical oilwell drill string. In this article the main task was to design a controller that would drive the bit velocity to the reference as fast as possible and maintain it without any stick-slip oscillations [36]. They applied three reaching laws in the sliding mode in the drilling process. Then, the simulation results showed that the control laws were capable of controlling the bit speed, had faster dynamic responses and suppressed stick-slip in oil well drill string [36]. After that, Qi-zhi *et al.* used the idea of introducing another surface discontinuity and forcing the system to evolve along this surface [37]. In this study the sliding-mode control was applied as described in their first article ([36]). They focused the analysis on a problem of linear time-variant system stability with time-delay.

Furthermore, some specific relationships between the former observer's gain and the delayed term was found with respect to the time delay through the Lyapunov's method.

Fubin *et al.* presented in 2010 the adaptive PID control strategy of the drilling system to eliminate the stick-slip phenomenon on the bit. The system is composed of two parts: the linearization method input controller and the adaptive PID controller [38]. The adaptive controller was designed to reduce or eliminate the problem caused by the fixed control parameters. Otherwise, when internal characteristics and external disturbances change in large scale, the system performance usually falls substantially [38]. Furthermore, the simulation results showed that this controller had good control characteristics and fast dynamic response. It could eliminate stick-slip oscillation of the drill bit and improve the performance of rotary table [38].

The model-based control approach also was largely used as a robust control strategy to control the drill string vibrations. Puebla and Alvarez-Ramirez (2008) [39] were one of the first to design a model-based controller. Basically, they used two control configuration to guarantee the system robustness: the called cascade control scheme and decentralized control scheme, both applied to numerical simulations. In their study they considered a 2-DOF system and several bit-rock interaction models in four different case studies.

Johanessen and Myrvold (2010) [40] seem to be the first to use the MPC (a model-based controller) to control the stick-slip behavior. They used the Nonlinear MPC (NMPC) approach to address the problem in a numerical drilling system. Also, they compared this strategy to the SoftSpeed device to prove the robustness of the developed system. Breyholtz (2012) [41] also cited the MPC as a good alternative to control the pressure during drilling operations. He advocates for its use in other applications. This study was based on the **Modes of Automation**, defined as the different levels of automation strategy using human-machine interactions.

Vromen (2015) [42] affirmed that the existing industrial controllers were deficient to control systems under the increasingly challenge operational condition. Then, he described two main reasons for this deficiency. First, the influence of multiple dynamical modes of the drill string for torsional vibrations. Next, the uncertainty in the bit-rock interaction. Therefore, to eliminate the vibrational effects in the drilling system controllers were designed and experimentally validated. The dynamic model adopted a bit-rock interaction model, with severe velocity-weakening effect, and the controller design were based on a lumped-parameter model, exhibiting the most dominant torsional flexibility modes and based on a finite-element method representation of a realis-

tic drilling system with a multi-modal model of the torsional dynamics. Two controller design methodologies that meet these requirements have been developed. The first is based on nonlinear observer-based controller synthesis approach for Lur'e-type systems with discontinuities. The second controller design strategy is based on the robust H_∞ -control. Moreover, these active controllers had been applied to an experimental setup designed and realized by the author. Also, he applied passive down-hole tools for stick-slip suppression.

2.3

Preliminary concepts

In this section some basic drilling associated terminologies will be presented. This terminology and methodology can be used on any other control strategies. Also, it presents introductory concepts of control systems as they are applied on further investigation. These control strategies are those that best fitted the subject of this study. Moreover, brief illustrations on graphical block diagrams are presented related to each control law.

2.3.1

Basic control definitions

2.3.1.1

Dynamical system

Several references has minutely described the full control theory for different applications and control strategies, such as [43, 44, 45, 46, 2]. Nevertheless, general elements of control are discussed and presented in this section, such as the elements of a general system, illustrated in Fig. 2.1.

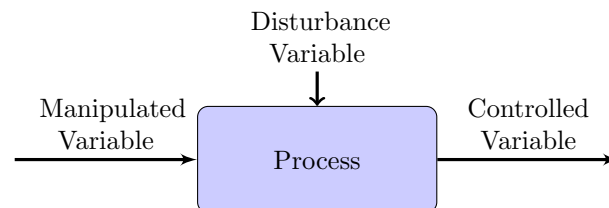


Figure 2.1: Block diagram representing a general System.

A system can be, generally, defined as a combination of elements and devices that act together to perform a certain objective. Although the possibility of applying this concept to many different dynamical phenomena, even abstracts such as those encountered in economics, the current study investigates the behavior of a dynamical mechanical system: the drilling system.

The corresponding dynamical system may be described with the physical elements of the drilling system illustrated in Fig. 1.1. This physical system will have its behaviors adequately described by mathematical models in Chapter 3.

In this study it is very important to notice that the actual drilling system is composed of controller plus actuator plus drill string, what strongly differs from the majority of several other studies.

For simplification, the full dynamical drilling system may be divided in two subsystems: DC motor subsystem and the drill string subsystem. Both systems together form a multivariable system that will be presented next. Moreover, both subsystems can be illustrated in a block diagram as two separated plants, defined by Ogata [46] as pieces of equipment or only sets of machine parts functioning together with the purpose of performing a particular operation.

Nowadays, the main objective of those subsystems/plants is still to perform the drilling process by means of the driller control action. Even considering all the innovation developed over the years. However, the driller has only control over three parameters at surface [47]: the hook-load (generates WOB); the surface rotary speed (SRPM); and the flow rate. These parameters are known as *manipulated variables*, also called control variables.

The driller also observes other three output parameters: the downward speed of the kelly (top end of the drill string when submitted to rotary table torque); the motor current of the rotary table or top drive; and the standpipe pressure. These parameters are the *controlled variables* that stand for the quantity or condition that is measured and controlled, usually maintained at some desired value referred to as *setpoint* or *reference* value. Moreover, for each controlled variable, there is an associated *manipulated variable* adjusted by the controller to keep the controlled variable value at or near their setpoint value.

To finalize the general system discussion, the *disturbance variable* is defined as the parameter that tends to drive the controlled variable away from the desired, reference or setpoint conditions. The disturbance can be internal (generated within the system) or external (generated outside the system). In the current case study, the main disturbance variable is the TOB, generated by the friction interaction between the drill bit and rock surface.

2.3.2

Open-loop and closed-loop systems

There are several distinctions between working with an open-loop drilling system and working with a closed-loop drilling system. Therefore, in order to elucidate these differences and other important aspects of the two system approaches, this section will discuss the details of each.

2.3.2.1

Open-loop system

First, the open-loop system and analysis are presented. Despite the simplicity of this application, it has not received the relevance it deserves over the last years. Only a few studies in the literature have realized the powerful tool that this analysis strategy can provide when used to understand behaviors of an unknown system. When talking about studies on drilling systems the number of studies is even smaller.

The open-loop system is especially beneficial to users because it provides more sensitivity and experience about the system being study, so, as consequence, they can develop increasingly robust control systems.

This strategy has notable features, such as the output signal without influence or effect on the controlled variable. Therefore, the open-loop system is known as a non-feedback system. This means that once the control strategy is set up, the output is neither measured nor fed back to compare with the input signal.

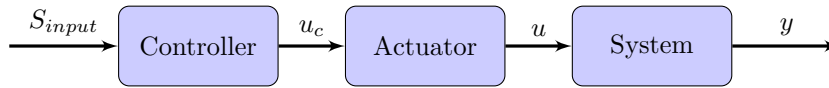
The current drilling process can be a good practical example of open-loop and manual control system when the driller does not take action on the system after it is in operation.

The elements of an open-loop system with and without control are represented in the block diagrams shown in Figs. 2.2.

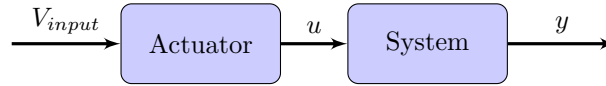
Generally, there are two open-loop system models: controlled or not controlled. In other words, for an open-loop analysis in a drilling system, the process may be equipped with a controller plus an actuator (Fig. 2.2(a)) or just with an actuator driven by an input signal 2.2(b). For the purpose of this study, the open-loop system is considered without the controller.

The S_{input} is the input signal of the controller in the block diagram of Fig. 2.2(a). The V_{input} and u_c are the voltage input signal of the actuator, the u is the torque input signal of the drilling system. The y is the output angular velocity of the drill string.

It is evident that if the drilling system is affected by the TOB or any other disturbance, there is a need for control. Therefore, to prevent errors



2.2(a): Open-loop system with feedforward control



2.2(b): Open-loop system without feedforward control

Figure 2.2: Block diagrams of open-loop systems.

from occurring due to disturbances, a control action (manual or automatic) should be applied. However, the open-loop analysis, to be performed in this study, will not have any type of disturbance because one of the objectives of this investigation is to understand the behavior of each dynamical system without any disturbance.

In summary, the main characteristics of an Open-loop System are defined as being [48]:

- There is no comparison between actual and reference values.
- An open-loop system has no self-regulation or control action over the output value.
- Each input setting determines a fixed operating position for the controller.
- Changes or disturbances in external conditions do not result in a direct output change¹.

2.3.2.2

Closed-loop system

The drilling process totally depends on the driller to inspect the, previously defined, *controlled variables* visually. As a result, he manages the *manipulated variables* [hook-load (WOB), SRPM, and flow rate] to adjust the process to achieve the setpoint value of the controlled variable. Therefore, when the driller takes action, he is manually closing the loop of the system.

The closed-loop system can use the same components presented in the open-loop system with controller (Fig. 2.2(a)). But the difference is the addition of one or more feedback loops. These loops may utilize actual angular velocity signal measurements and compare them with the desired angular velocity value (setpoint). These measures are called feedback signals and may be collected by a sensor or a transducer.

The difference between the setpoint and the actual angular velocity (by mean of feedback signal) generates an error signal. Then, this signal is treated

¹Unless the controller setting is altered manually

by the controller to obtain a control signal, also called the manipulated variable. Finally, the manipulated variable can be used to stabilize a disturbed dynamic system.

For this study the closed-loop analysis of the drilling process will be performed with disturbance and without disturbance. Furthermore, the closed-loop control system, also known as feedback control system, is represented by the block diagram shown in Fig. 2.3.

The Ω_{ref} is the reference signal of the system to be compared to the measured angular velocity y_m in the block diagram of Fig. 2.3 and generates the error signal $E(t)$. The U_m is the voltage input signal of the actuator, the T_m is the torque input signal of the drilling system. The y is the output angular velocity of the drill string.

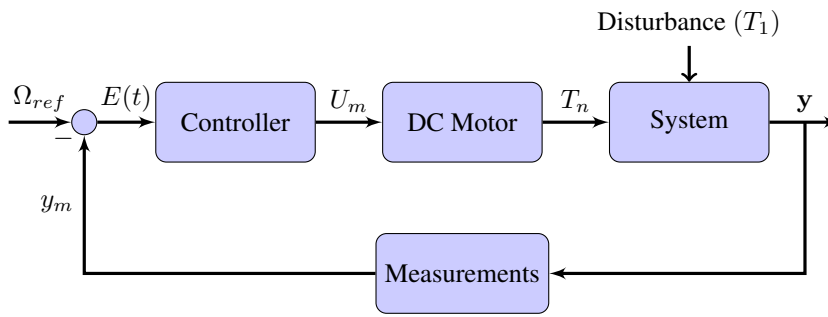


Figure 2.3: General block diagrams of a closed-loop system.

The feedback control systems are the most used control methodology of the industry. A quick literature review on stick-slip vibration control shows that the most part of the studies about the topic uses the feedback theory for analysis and design[20, 21, 49]. It is the simplest way to automate the control process by generating a control action dependent of the comparison between the output measured signal and the desired signal.

In summary, the main characteristics of Closed-loop Control are defined as being [50]:

- To reduce errors by automatically adjusting the systems input.
- To improve stability of a disturbed system.
- To increase or reduce the system sensitivity.
- To enhance robustness against external disturbances to the process.
- To produce a reliable and repeatable performance.

2.3.3

Automatic control systems

The previous sections discussed about the manner in which the automatic and manual controller produce the control signal using the feedback or feedforward control systems. Now, the control strategies used in the current study are discussed in more details. Well known industrial closed-loop controllers were chosen according to their control actions, such as:

- Proportional and integral controller (PI)
- Proportional, integral and derivative controller (PID)
- Model predictive control (MPC)

The cited controllers can be categorized according to general approaches related to control system design. Thus, this study focus on two of them [2]:

1. **Conventional approach.** The classical control strategies, such the PID-types, have been largely applied in oilwell industry using the feedback or feedforward laws. Therefore, the control system design can be developed based on this approach in a linear and nonlinear system. Moreover, once the control system is installed in the plant the *controller tuning* strategy can start to be applied.
2. **Model-based approach.** The model-based approach uses the dynamical model to predict the behavior of the drilling system by means of a mathematical model of the process (also called internal model). The suggested mathematical model has three possible applications: (i) it can be used as the basis for model-based controller design methods; (ii) it can be incorporated directly in the control law; (iii) the model can be used in a computer simulation to evaluate alternative control strategies and to determine preliminary values of the control settings [2].

Clearly, both approaches have strong industrial application. However, control strategies under the conventional approach are the most used in industrial processes. For example, Astrom (1994) [43] determined that more than 95% of the control loops were of PID type and most of this loops used PI control. In his turn, Breyholtz (2012) [41] determined that the PID controllers are by far the most widely used control technology in the oilwell industry.

On the other hand, if a conventional control system can not be satisfactory, an alternative approach, such as the model-based control, may be applied. In that case, this study intends to use the MPC as a sophisticated enough strategy to control the complex dynamical drilling system.

According to what Breyholtz (2012)[41] determined in his study: it is not necessary completely replacing human resources in the rig floor by autonomous

systems. However, the automation must improve performance during normal drilling operations while allowing the driller to intervene in varying degrees in case of abnormal events.

2.3.4

Proportional, integral and derivative actions and controllers

To apply any control action in the closed-loop drilling system, the Controller box (see Fig. 2.3) can be replaced by a well defined classical strategy such as P, PI, PD, PID controller (or a combination of them). Each P,I and D actions and two control strategies (PI and PID) will be presented in this section to adjust the angular velocity parameter.

Even when referring to stick-slip active control, the PID controller is said to be the "bread and butter" of control engineering. Hence, this simple controller has become a test bench for many new ideas in control and it has proved its utility with a satisfactory performance when compared with other developed strategies.

2.3.4.1

Proportional action

The Proportional feedback controller is defined as the control signal made to be linearly proportional to the error signal for small errors. Thus, the proportional controller can be seen as an amplifier that adjust the gain up to the desired velocity. However, this controller may cause a static or steady state error in response to a constant velocity setpoint and may not be capable, by itself, to eliminate the disturbance completely.

2.3.4.2

Integral action

The integral action is the one responsible for improving the steady state accuracy (by eliminating the error) of a control system under the proportional action. So, it makes sure that the controlled variable agrees with the velocity setpoint in steady state. However, at the end of the process the integral action can cause a worse transient response.

2.3.4.3

Derivative action

The derivative action is an important tool to improve the closed-loop stability. On this action of control the magnitude of the controller signal is proportional to the rate of range of the actuating error signal. Besides its

anticipatory characteristics, this action can never anticipate an action that has not yet taken place.

2.3.4.4

Proportional and integral controller (PI)

The principle used in the SoftTorque control system (PI controller) is based on the proportional and integral control theory. The same used in the current study. However, the only difference is the use of the DC motor dynamic on the full scale system modeled here. The PI control strategy is also known as the standard velocity controller and it is applied to correct the error between the actual and desired angular velocity of the top drive actuator (rotating motor) on the drilling system.

So, based on the PI actions described in this section and on the general block diagram of Fig. 2.3, the mathematical control law has the form:

$$\begin{aligned} \mathbf{u}_c(t) &= k_p [r(t) - y_m(t)] + k_i \int_0^t [r(t) - y_m(t)] dt \\ &= k_p e(t) + k_i \int_0^t e(t) dt \end{aligned} \quad (2-1)$$

where u_c is the control signal, y_m is the controlled variable, r is the manipulated variable and e is the control error ($e = [r(t) - y_m(t)]$). k_p is the proportional gain. k_i is the integral gain and can be represented as $k_i = \frac{k_p}{T_i}$. T_i is the integral time constant.

2.3.4.5

Proportional, integral and derivative controller (PID)

Several applications of PID control has been applied to the dynamical drilling system, as seen in the references [38, 36, 41, 51]. But few of them have used the controller plus actuator in their dynamical system, as is used in the current study. As discussed before, the PID control has three terms with specific characteristics that combined provides the classical PID control strategy. Some of the advantages and disadvantages are:

(P) - Proportional:

Advantage - It reduces error response to disturbance and increase the speed of response.

Disadvantage - It has a much larger transient overshoot [45].

(I) - Integral:

Advantage - It can eliminate the steady-state error.

Disadvantage - It costs the deterioration in the dynamic response.

(D) - Derivative:

Advantage - It damps the dynamic response and improves the closed-loop stability.

Disadvantage - It is late in correcting for an error.

In summary, the most used control method provides feedback, eliminates steady-state error through integral action, and anticipates the future through derivative action [43].

The mathematical representation of the PID controller is based on the proportional, integral and derivative actions, described in previous sections, which has the form:

$$\begin{aligned} \mathbf{u}_c(t) &= k_p [r(t) - y_m(t)] + k_i \int_0^t [r(t) - y_m(t)] dt + k_d \frac{d}{dt} [r(t) - y_m(t)] \\ &= k_p e(t) + k_i \int_0^t e(t) dt + k_d \frac{d}{dt} e(t) \end{aligned} \quad (2-2)$$

where u_c is the control signal, y_m is the controlled variable, r is the manipulated variable and e is the control error ($e = [r(t) - y_m(t)]$). k_p is the proportional gain, k_i is the integral gain and k_d is the derivative gain. $k_i = \frac{k_p}{T_i}$, $k_d = k_p T_d$. The T_i is the integral time constant and the T_d is derivative time constant.

2.3.5

Model predictive control (MPC)

Among the various model-based control laws previously presented (see section 2.2) this study focuses on the MPC as the strategy to deal with complex dynamic drilling systems. The strategy works when a reasonable accurate drilling dynamic model is available. Hence, the MPC design was chosen due to two main characteristics: it deals naturally with multivariable control problems and allows the system to operate closer to its constraints [2].

Fig. 2.4 exposes the flowchart with the major steps to design and install a control system using the model-based approach [2].

The MPC system is illustrated in the block diagram in Fig. 2.5. It is a feedback control law that uses the outputs of a well-defined dynamic *Model* and the current measurements of the drilling *Process* to predict the future values of the output variables, such as angular velocity. The comparison between the actual (*Process outputs*) and *Model outputs* generates the feedback signal called *Residuals* to feed the *Prediction* block. The *Prediction* block uses an optimization algorithm to predict these variables. This optimization is

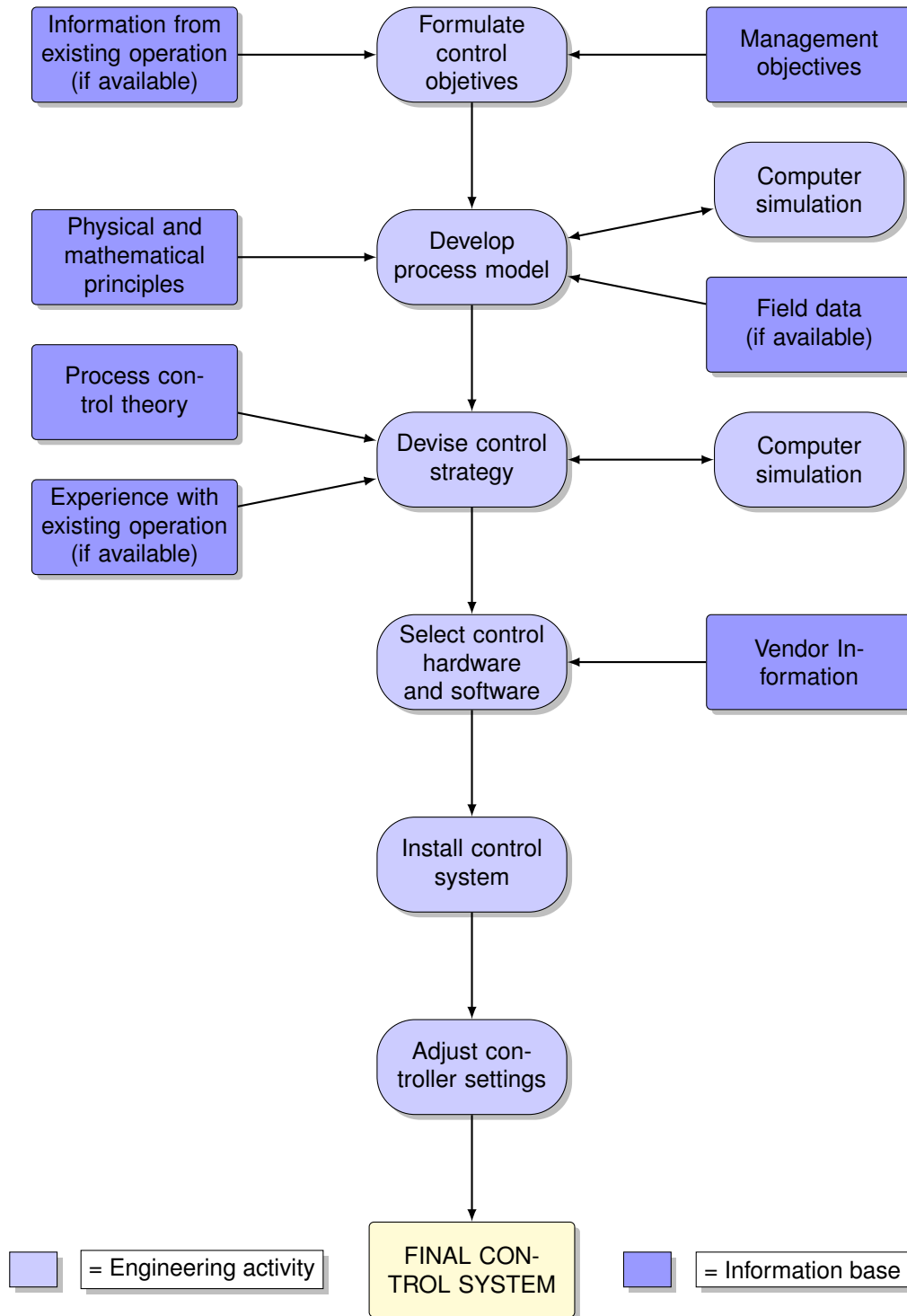


Figure 2.4: Major steps in model-based control design. (Adapted from Seborg (2004) [2]).

performed at each time step with the same horizon and uses the updated measures/estimates of states and the disturbances. Predicted output values feed the *Setpoint calculations* and *Control calculation*. These boxes generate the *Input* variables. Also, system constraints, such as upper and lower limits,

can be considered at each time step during performance [2, 40].

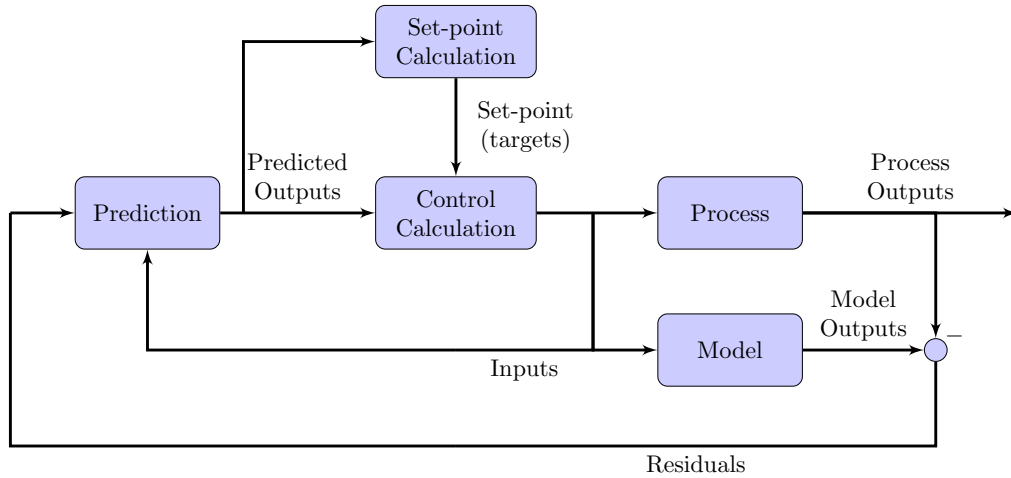


Figure 2.5: Block diagram for MPC. (Adapted from Seborg (2004) [2]).

The MPC system application provides benefits, such as:

- Prevent violations of input and output constraints.
- Directs the output variables to their optimal setpoints while maintaining other outputs within specified ranges.
- Prevents excessive movement of input variables.
- Controls as many variables as possible when a sensor or actuator is unavailable.

The control calculations are based on current measurements and predictions of the future values of the outputs. The predictions are made using, typically, a linear dynamic model. But for very nonlinear processes, it can be advantageous to predict future outputs values using a nonlinear dynamic model [2].

The purpose of the MPC control calculations is to determine a sequence of *control movements* to move the predicted response to the setpoint optimally. An illustration of what occurs when a MPC is applied can be seen in Fig. 2.6. At the moment of current sampling, denoted by k_t , the MPC strategy calculates a set of M values of the input $\{u(k_t + i - 1), i = 1, 2, \dots, M\}$. The set consists of the current input $u(k_t)$ and $M - 1$ future inputs. The inputs are held constant after the M control moves. The inputs are computed so that the set of P predicted outputs $\{\hat{y}(k_t + i), i = 1, 2, \dots, P\}$ reaches the setpoint optimally. The number of predictions P is referred to as *prediction horizon* while the number of control moves M is called *control horizon* [2].

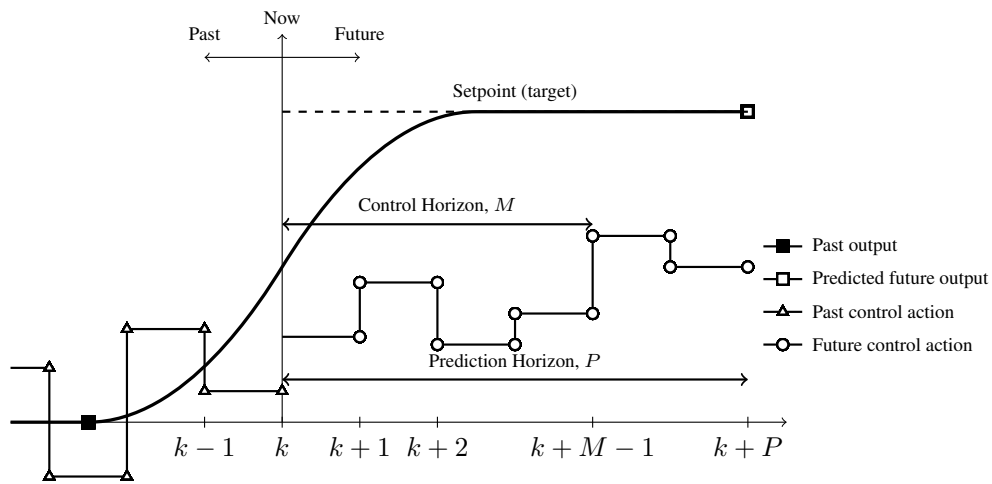


Figure 2.6: Basic concept for MPC. (Adapted from Seborg (2004) [2]).

3

Mathematical modeling of the dynamical drilling system

3.1

Introduction

One of the key role in the model-based control design is the development of a dynamic model of the drilling process, as mentioned in Fig. 2.4. The theoretical model is developed based on physical and mathematical principles to simulate the dynamic torsional system in order to provide insights into system behavior. This dynamic is based on a simplified drilling system model (only 2-DOF), considering some assumptions and including operational model parameters of a realistic full-scale system.

This chapter is concerned with the development of the torsional dynamic model of the drilling system. For that propose, first, the dynamic modeling and the corresponding equation of motion are derived. In this step, the influence of some drilling components, such as top drive unit, drill pipes, BHA and drill bit, on the system behavior will be considered. Then, the state-space equation of the electromechanical system is presented as a combination of the torsional drill string and DC motor dynamic models. Finally, the friction model used to generate the stick-slip is presented.

3.2

Dynamic modeling

3.2.1

Modeling approach: two degrees of freedom

The rotary system is the most used method for drilling wells in the oil and gas industry. In the last few years, the oil industry process development promoted the top drive unit to the top of the list of the preferred drive systems used in the drilling operations. A simple schematic of the full scale drilling system is illustrated in Fig. 3.1.

To simplify the model analysis some considerations will be assumed, e.g., the borehole is a vertical trajectory. Also, the lateral and axial motions of the drill bit will not be considered. Thus, the current study deals only with torsional vibrations modes of the drill string. Although the various ways to represent the

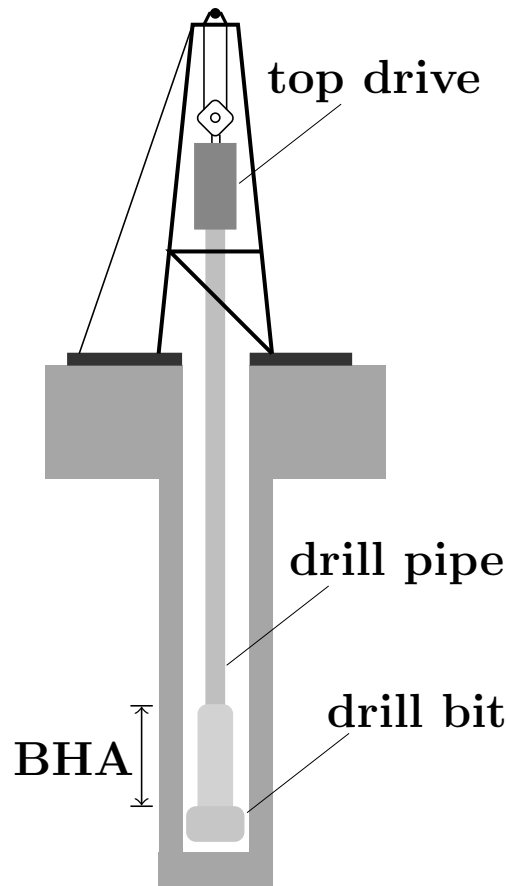


Figure 3.1: Schematic of modern drilling system.

dynamic of the drill string (e.g., **i** - one-mode [12]; **ii** - beam model with the finite element method (FEM) [13]; **iii** - discrete system with one, two or more DOF [34, 52]) it was chosen for this study a discrete 2-DOF system because of its intuitive ease to be implemented in a numerical simulation.

The torsional drilling process will be divided in two dynamic subsystems: the *upper system* and the *lower system*. The first part (upper), acting as a flywheel, is driven by a DC motor, represented by the top drive unit that delivers torque on the surface. The upper dynamic has a considerable impact on the full dynamical behavior. On the other hand, the lower part consists of drill pipes, BHA and a drill bit. Both subsystems are physically connected to perform the drilling operation. Therefore, both dynamics will be investigated here.

3.2.1.1

Lower system: torsional pendulum

Although the importance given to the upper system modeling in this study (see section 3.2.1.2), the main physical behavior occurs in the lower system. For example, the stick-slip phenomenon disturbs measurements done

by components of the lower system while drilling. Therefore, the torsional vibration control has a crucial role for the accuracy of the modeling of this system.

Furthermore, it can be noticed from the literature about stick-slip vibrations that a great part of the studies only consider the lower system in their dynamical modeling. Those characteristics make this dynamical system the most relevant part to approach the torsional vibration problem.

Fig. 3.2 illustrates the drill string dynamical model. It assumes that the lower system behaves as a torsional pendulum when drilling. So, the torsional drilling dynamics can be modeled as a two DOF system, for simplicity. Moreover, constant WOB and a reference angular velocity (Ω_{ref}) are imposed on the surface inertia (J_2). The model can be considered very simple in comparison to the different models presented in literature and since the 2-DOF represents only few specific realistic situations, but it is an important step for the purpose of this study.

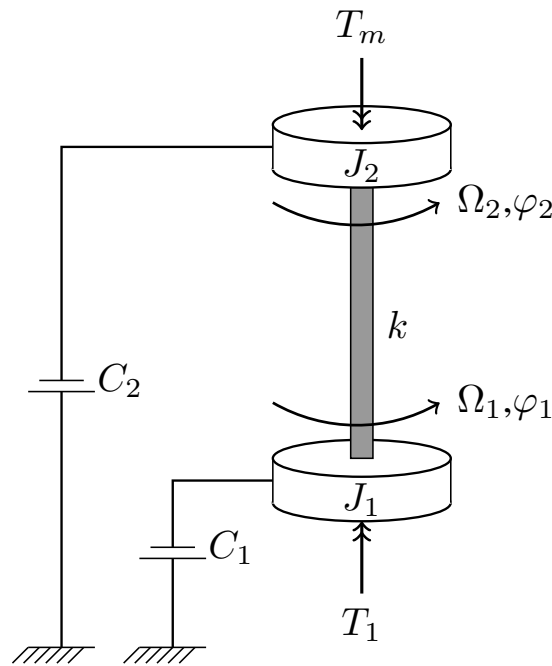


Figure 3.2: A drill string system modeled as a torsional pendulum.

The two DOF model was also used by Cayres (2013) [52] in his study. Thus, the model consists of two damped inertia mechanically coupled by an elastic drill string where the surface torque (STOR) T_m is imposed by a motor at the top end, as shown in Fig. 3.2. The drill string is homogenous along its entire length and considered as a single linear torsional spring with stiffness coefficient k [38, 36]. The main variables observed for this analysis are the

Surface RPM (SRPM) Ω_2 and the Downhole RPM (DRPM) Ω_1 measured on the top drive and on the BHA, respectively.

The corresponding equations of motion of the drill string system are represented by the model of torsional dynamics in Eq. 3-1.

$$\begin{bmatrix} J_1 & 0 \\ 0 & J_2 \end{bmatrix} \begin{bmatrix} \dot{\Omega}_1 \\ \dot{\Omega}_2 \end{bmatrix} + \begin{bmatrix} C_1 & 0 \\ 0 & C_2 \end{bmatrix} \begin{bmatrix} \Omega_1 \\ \Omega_2 \end{bmatrix} + \begin{bmatrix} k & -k \\ -k & k \end{bmatrix} \begin{bmatrix} \varphi_1 \\ \varphi_2 \end{bmatrix} = \begin{bmatrix} -T_1 \\ T_m \end{bmatrix} \quad (3-1)$$

where φ_1 and φ_2 are the angular displacements of the BHA and the top drive, Ω_1 and Ω_2 are the angular velocities measured at the downhole and surface positions. J_1 and J_2 are the equivalent mass moment of inertia of the BHA and of the upper system (a combination of the drill pipes and the surface component such as drive motor, gear box and top drive). C_1 and C_2 are the equivalent viscous damping coefficients, k is the equivalent torsional stiffness of the drill pipe, and T_1 is the nonlinear function representing the downhole torque on bit (TOB).

$$J_1 = \rho_{bha} I_{bha} L_{bha} \quad (3-2)$$

$$J_2 = \rho_{dp} I_{dp} L_{dp} \quad (3-3)$$

where L_{dp} and L_{bha} are the lengths of the components. ρ_{bha} and ρ_{dp} are the mass densities. I_{dp} and I_{bha} are the area moments of inertia for the drill pipe and the BHA, respectively. They can be written as:

$$I_{bha} = \frac{\pi}{32} (OD_{bha}^4 - ID_{bha}^4) \quad (3-4)$$

$$I_{dp} = \frac{\pi}{32} (OD_{dp}^4 - ID_{dp}^4) \quad (3-5)$$

where OD_{bha} and OD_{dp} are the outer diameters. ID_{bha} and ID_{dp} are the inner diameters.

The equivalent viscous damping coefficients (C_1, C_2) are written in terms of the damping factor of the mud Dr ,

$$C_1 = Dr L_{bha} \quad (3-6)$$

$$C_2 = Dr L_{dp} \quad (3-7)$$

The torsional stiffness of the drill pipe is:

$$k = \frac{G I_{dp}}{L_{dp}} \quad (3-8)$$

where G is the shear modulus $G = \frac{E}{2(1+\nu)}$. E is the Young's modulus and ν is the Poisson ratio.

For this simple two DOF modeling, the matrix of inertia $\{\mathbf{J}\}$, damping $\{\mathbf{C}\}$, and stiffness $\{\mathbf{K}\}$ from Eq. 3-1 are illustrated as follows:

$$\{\mathbf{J}\} = \begin{bmatrix} J_1 & 0 \\ 0 & J_2 \end{bmatrix}, \{\mathbf{C}\} = \begin{bmatrix} C_1 & 0 \\ 0 & C_2 \end{bmatrix}, \{\mathbf{K}\} = \begin{bmatrix} k & -k \\ -k & k \end{bmatrix}$$

3.2.1.2

Upper system: DC motor

The main difference between the model presented in Cayres [52] (and several other studies) and the model studied here is the implementation of the electrical equations of the top drive motor, first presented by Jansen *et al.* [25]. The electric circuit of the armature and the free-body diagram of the rotor are shown in Fig. 3.3. The behavior of the DC electronic motor has its dynamical principles represented by two linear models: (1) The mechanical equation of free-body diagram of the rotor. (2) The electric circuit equation of armature.

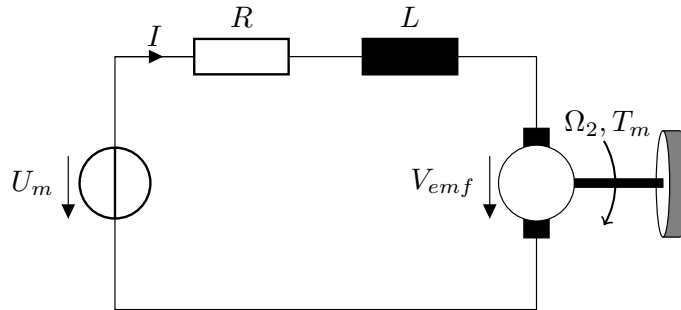


Figure 3.3: Electrical equivalent circuit of armature.

The equation of motion of the rotor has already been presented in Eq.3-1, but it is modified based on the Kirchhof's law and Newton's Second law. Therefore, it is assumed that the magnetic field is constant and the torque is directly proportional to the armature current I . By this time, the armature current is the electric variable of DC motor and the angular velocity is the mechanical variable as presented in the reduced linear equations below.

$$L \dot{I} + RI + V_{emf} = U_m \quad (3-9)$$

$$V_{emf} = k_e \Omega_2 \quad (3-10)$$

$$T_m = k_t I \quad (3-11)$$

where I is defined as armature current. R and L are electrical resistance and electrical inductance, respectively. U_m is the motor input voltage. V_{emf} represents the back-electromotive force (back-emf) related to the angular velocity Ω_2 . k_e and k_t parameters are respectively the electromotive force constant and the motor torque constant.

3.2.2

State-space equation of the electromechanical system

By substituting the motor torque and the back-emf (3-10) in the Eqs. 3-1 and 3-9 and rearranging both together, the state-space equation of electromechanical system can be expressed as:

$$\mathbf{q}' = \{\mathbf{A}_1\}\mathbf{q} + \{\mathbf{A}_2\}u + \mathbf{T} \quad (3-12)$$

$$\mathbf{y} = \{\mathbf{A}_3\}\mathbf{q} \quad (3-13)$$

where \mathbf{q} is the state vector, $\{\mathbf{A}_1\}$ is the set parameters coefficient matrix, $\{\mathbf{A}_2\}$ the input parameter vector controlled by the scalar control law u , \mathbf{T} is the torque disturbance vector, $\{\mathbf{A}_3\}$ is the output parameter matrix, and \mathbf{y} is the output vector.

Thus, the state-variables are written in matrix form as:

$$\mathbf{q} = \begin{bmatrix} \varphi_1 \\ \varphi_2 \\ \Omega_1 \\ \Omega_2 \\ I \end{bmatrix}, \quad \{\mathbf{A}_1\} = \begin{bmatrix} 0 & 0 & 1 & 0 & 0 \\ 0 & 0 & 0 & 1 & 0 \\ -\underline{\mathbf{J}}^{-1}\underline{\mathbf{K}} & -\underline{\mathbf{J}}^{-1}\underline{\mathbf{C}} & 0 & 0 & 0 \\ 0 & 0 & 0 & -k_e/L & -R/L \end{bmatrix}, \quad \mathbf{T} = \begin{bmatrix} 0 \\ 0 \\ -T_1/J_1 \\ T_m/J_2 \\ 0 \end{bmatrix},$$

$$\mathbf{y} = \begin{bmatrix} y_1 \\ y_2 \\ y_3 \\ y_4 \\ y_5 \end{bmatrix}, \quad \{\mathbf{A}_2\} = \begin{bmatrix} 0 \\ 0 \\ 0 \\ 0 \\ 1/L \end{bmatrix}, \quad \{\mathbf{A}_3\} = \begin{bmatrix} 0 & 0 & 0 & 0 & 0 \\ 0 & 0 & 0 & 0 & 0 \\ 0 & 0 & 1 & 0 & 0 \\ 0 & 0 & 0 & 1 & 0 \\ 0 & 0 & 0 & 0 & 0 \end{bmatrix}$$

As the initial conditions of the dynamic system will be considered only the torsional behavior, the surface and downhole angular velocities and displacements are zero.

3.2.3

Friction torque modeling

The nonlinear resistive torque at the bit properly modeled based on a cutting process model because of the characteristic of the bit-rock interaction.

But for simplicity it can be modeled for a friction law T_1 depends on the WOB, the friction coefficient μ and the friction factor $P_f(\Omega_1)$ (dependent on the velocity). The function covers static (P_{f-s}) + Coulomb (P_{f-c}) + approximation of negative damping (P_{f-nd}) regions. The composite function tries to simulate the friction model based on the nonlinear bit-rock interaction.

In the literature, it is easy to find references of the friction models, such as cited by Germay *et al.* [53] and with different degrees of complexity such as Karnop and LuGre models [54, 55]. Based on that, the most common friction models are presented below, including:

- (a) Velocity weakening laws [56],
- (b) Stiction plus Coulomb friction [7, 26],
- (c) *Stribeck effect*¹

The corresponding friction law can cause torsional vibrations in the drill string system. To better emulate this behavior in the model the relation is assumed to be practical, nonlinear, and suitable for dynamic analysis and controller synthesis. The practicality of the model is observed when:

- It reproduces the required phenomenon (stick-slip);
- The model presented is as simple as possible and fast to implement on numerical analysis.

For this reason, the Eq. 3-14 describes how the resistive torque at the drill bit is modeled based on the following friction law.

$$T_1 = \mu \cdot WOB \cdot P_f(\Omega_1) \quad (3-14)$$

where μ is a constant friction coefficient, WOB is the weight on bit, also constant in the model, and $P_f(\Omega_1)$ is the velocity-dependent proportional friction factor.

The set-valued proportional friction factor law is modeled as a composition of others literature models and has been suited to generate stick-slip behavior under specific conditions.

$$P_f(\Omega_1) = \begin{cases} P_{f-s}, & \text{for } \Omega_1 < Tol \\ P_{f-nd}, & \text{for } Tol \leq \Omega_1 < \Omega_{dyn} \\ P_{f-c}, & \text{for } \Omega_1 \geq \Omega_{dyn} \\ P_{f-neg}, & \text{for } \Omega_1 < 0 \end{cases} \quad (3-15)$$

¹Characterized by a decreasing friction-velocity map localized around zero velocity.

where P_{f-s} , P_{f-c} are described in table 3.1. The negative damping approximation is described by the general relation $P_{f-nd} = \alpha\Omega_1 + \beta$ (being $\alpha = -0.076$ and $\beta = 1.3$). Tol is a stipulated speed tolerance ($Tol = 0.01$) and Ω_{dyn} is the final speed of the sticking regime ($\Omega_{dyn} = 8.5 \text{ rad/s}$). P_{f-neg} is a “negative” friction factor when the angular velocity reaches negative values.

The complete set-valued friction model is shown in Fig. 3.4 and the coefficients considered, as presented in Eq. 3-15, are defined in Tab. 3.1.

Factor	Description	Value	Setpoints [rad/s]
P_{f-s}	Static factor	1.30	0.01
P_{f-c}	Coulomb factor	0.65	8.50
P_{f-neg}	”Negative” factor	-0.20	≤ 0

Table 3.1: Friction factors values used in the friction modeling.

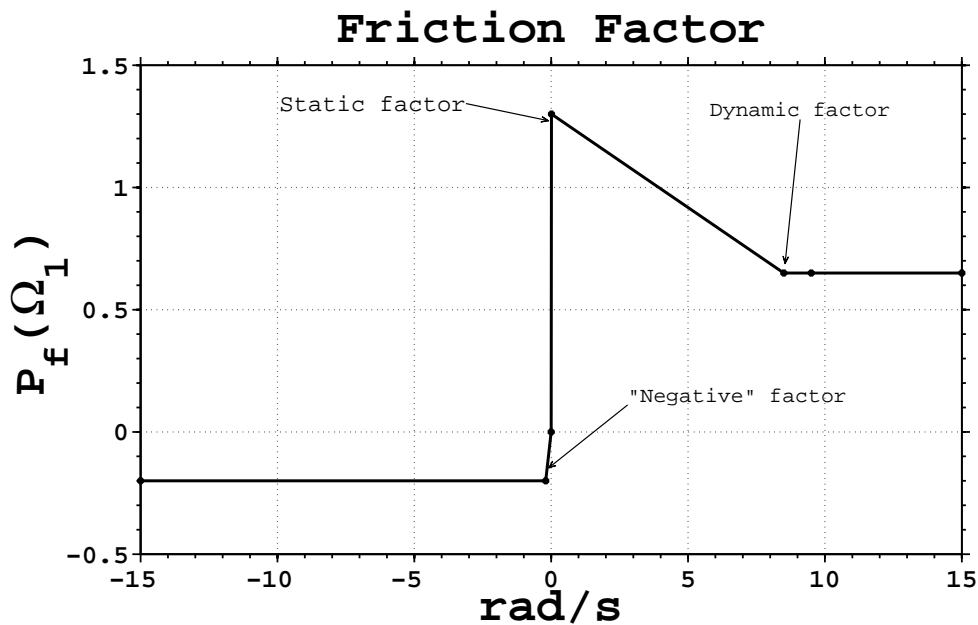


Figure 3.4: Static + Coulomb + Negative damping friction model.

4

Control design: open-loop and closed-loop approaches

4.1

Introduction

This chapter presents the open-loop and closed-loop systems for a set of input parameters, analyzing the application of some different types of control laws used to control the drill string torsional vibration. Thus, the focus of these control strategies are to mitigate the torsional vibrations acting on surface to achieve at the drill bit. Additionally, this chapter evaluates which of the controllers could be “a good choice” for a real-time implementation.

4.2

The open-loop analysis

In the stick-slip control literature (in Section 2.2) it is observed that great part of the cited studies focused on the closed-loop approach. Although the importance of this closed-loop analysis for the final control design, the open-loop analysis may be a robust (in terms of control stability) tool to help decision making in order to improve control performances. Also, it is important to make a distinction between the actual research from the others: here, the system is composed of a combination of the electromechanical motor dynamics and the drill string dynamics.

In this section, the open-loop analysis is performed, first, by un-looping the feedback system and, then, analyzing both dynamical components separately.

Basically, the closed-loop control system (see Fig. 4.1) compares the measured surface angular velocity Ω_2 to the reference angular velocity Ω_{ref} and, then, the error signal $E(t)$ is generated. Next, this signal is manipulated by the controller to provide the supply voltage U_m (control signal) that activates the DC motor. In its turn, the DC motor delivers the motor Torque T_m that drives the drilling system by providing rotary motion. The studied closed-loop system is composed of a controller and two subsystems: DC motor and drill string.

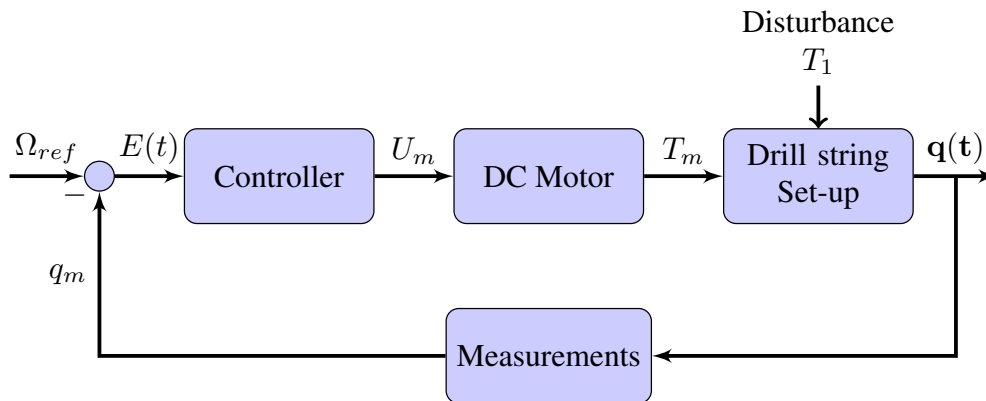


Figure 4.1: Block diagram of the closed-loop drilling system.

The proposed methodology allows a better understanding of how the subsystem impacts in the dynamics of the full drilling system. Also, this methodology provides the system characterization, thoroughly. For that purpose, some different scenarios will be performed.

Basically, simple open-loop step responses are performed to investigate the influence of the subsystems described earlier. Consequently, two simple dynamical models¹ are considered separately (based on the Eqs. 3-1-3-11). The steps in the open-loop analysis are summarized as following:

- Step 1** - Ignore any disturbances considered in the system;
- Step 2** - Eliminate the comparison between the actual angular velocity Ω_2 and the reference angular velocity Ω_{ref} ;
- Step 3** - The controller is disregarded from the system once the feedback measure is eliminated;
- Step 4** - The two main subsystems¹ are separated.

This methodology is graphically illustrated in Fig. 4.2, resulting in the two open-loop subsystems.

According to Fig. 4.2, after excluding the feedback loop, the DC motor actuator is the first open-loop subsystem presented, as seen in Fig. 4.3. In this case, the motor is modeled as a single electromechanical system composed of an electric circuit of the armature (Eqs. 3-9-3-11) with the free-body diagram of the rotor (surface inertia J_2). Therefore, the input-output form of the DC motor system is expressed in terms of the input voltage U_m (and its derivative) and the output is the torque (T_m) delivered by the motor. The torque is related to the armature current $I(t)$, as explained in the model of Section 3.2.1.2.

¹motor actuator model and drill string model

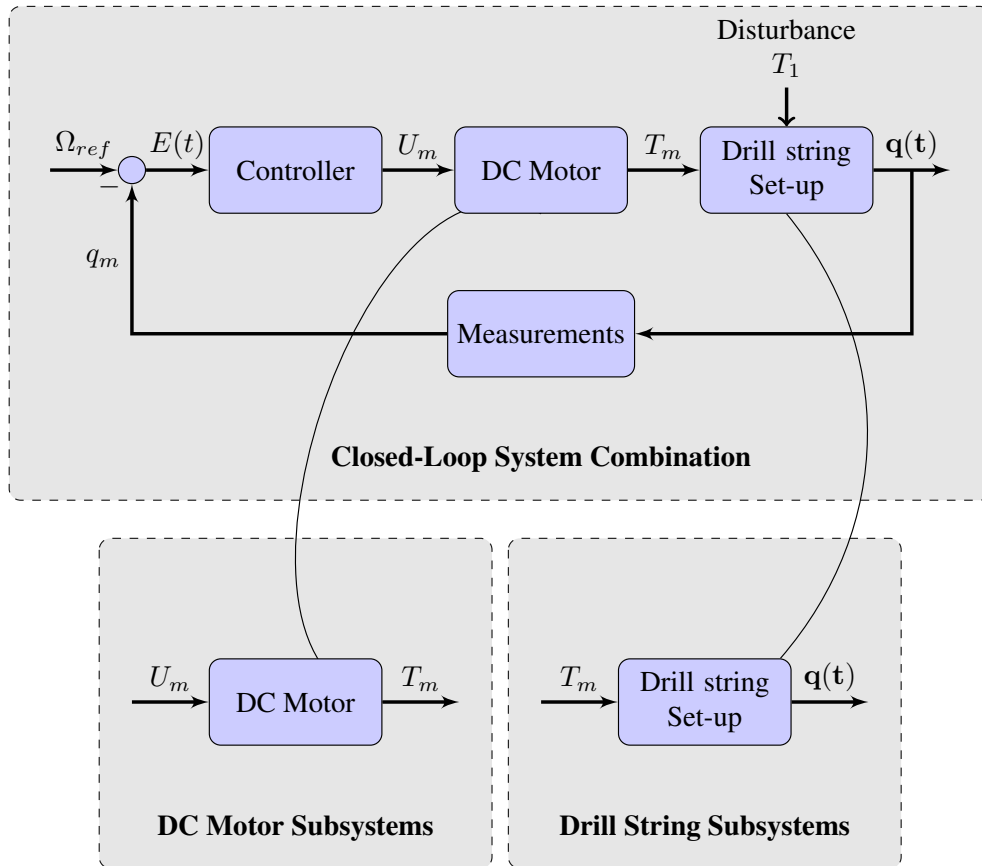


Figure 4.2: Process of opening the loop of the drilling system.

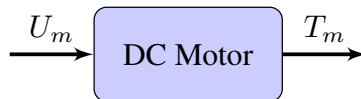


Figure 4.3: Block diagram of the open-loop DC motor.

Similarly, the open-loop analysis derives the drill string dynamic subsystem. As assumed earlier, the subsystem is not affected by disturbances. Thus, applying the previous methodology opening the loop, the drill string can be modeled as a 2-DOF body diagram where the input is the torque action (T_m) on the surface and the output is the angular velocity vector ($\mathbf{q}(t)$), as illustrated in Fig. 4.4.

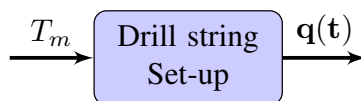


Figure 4.4: Block diagram of the open-loop drill string.

4.2.1

Mathematical simplifications for the open-loop analysis

Figs. 4.3 and 4.4 illustrate the equivalent actuator and the plant of the closed-loop system, seen in Fig. 4.1. Both subsystems have some important mathematical simplifications that can be done. The drill string dynamic system is analyzed first, due to the expected contribution of its components on the full dynamic system performance. However, the only simplification when performing the analysis on the drill string subsystem is the motor torque T_m without disturbances. Furthermore, the nonlinear torque on bit T_1 is assumed to be null. On the other hand, the input torque delivered by the DC motor to the drill string reveals the relevance of the upper system components on the full system dynamics.

To obtain consistent responses in the simulations, sensitivity analyzes are performed in both subsystems. These analyzes consist of applying a range of input torques T_m on the drill string system and observing the angular velocities achieved. Then, a computer interaction performs the same range of torque (as reference) in order to achieve the applied supply voltage in the DC motor subsystem. As a consequence, the surface angular velocity Ω_2 achieved on the drill string is associated to a torque, set in the DC motor subsystem. Therefore, rewriting the Eqs. 3-1 - 3-11 based on the assumed simplifications, the equation of motion of the open-loop drill string subsystem in state-space form is expressed as:

$$\begin{bmatrix} \dot{\phi}_1 \\ \dot{\phi}_2 \\ \dot{\Omega}_1 \\ \dot{\Omega}_2 \end{bmatrix} = \begin{bmatrix} 0 & 0 & 1 & 0 \\ 0 & 0 & 0 & 1 \\ -\mathbf{J}^{-1} \begin{bmatrix} k & -k \\ -k & k \end{bmatrix} & -\mathbf{J}^{-1} \begin{bmatrix} C_1 & 0 \\ 0 & C_2 \end{bmatrix} \end{bmatrix} \begin{bmatrix} \phi_1 \\ \phi_2 \\ \Omega_1 \\ \Omega_2 \end{bmatrix} + \begin{bmatrix} 0 \\ 0 \\ T_1 \\ T_m \end{bmatrix} \quad (4-1)$$

$$\mathbf{y}_1 = \begin{bmatrix} 0 & 0 & 1 & 0 \\ 0 & 0 & 0 & 1 \end{bmatrix} \begin{bmatrix} \phi_1 \\ \phi_2 \\ \Omega_1 \\ \Omega_2 \end{bmatrix} \quad (4-2)$$

and the Eq. of motion of the DC motor subsystem is given bellow

$$\dot{I} = \frac{-1}{L}[RI + k_e \Omega_2] + U_m \quad (4-3)$$

$$T_m = k_t I \quad (4-4)$$

Remembering: $T_1 = 0$, T_m is the input torque and Ω_2 is the surface angular velocity.

4.3

Closing the loop

It is a consensus that state feedback control improves system performance if compared with the open-loop implementation. In this sense, the closed-loop system is, first, performed without disturbances and expecting linear output responses. In addition, the actuator (DC motor) and the plant (drill string) are assumed combined in the full system with the feedback controller.

In this study, the objective of the feedback strategy is to control the angular velocity of the top drive and the BHA. For this propose, the same methodology explained in the third paragraph of the Section 4.2 is considered in this analysis. Thus, the current feedback closed-loop control is represented by the block diagram illustrated in Fig. 4.5.

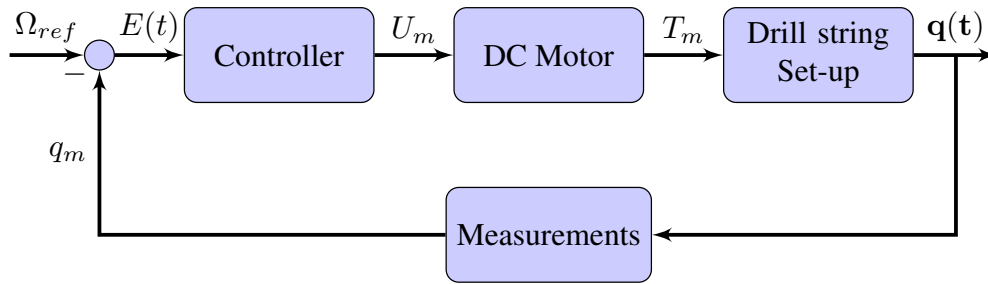


Figure 4.5: Block diagram of the closed-loop drilling system without disturbance.

First, the PID controller (known as the standard top rotary speed controller[11]) is adopted for comparison with the open-loop results. The goal of this control action attempts to maintain the angular velocity in a constant setpoint without disturbances in the system [57].

The control strategy delivery supply voltage to the DC motor using the following PID control law:

$$U_m(t) = k_p E(t) + \frac{k_p}{T_i} \int_0^t E(t) dt + k_p T_d \frac{dE(t)}{dt} \quad (4-5)$$

where k_p , $k_i = \frac{k_p}{T_i}$, and $k_d = k_p T_d$ are, respectively, the proportional and integral control parameters. $U_m(t)$ is the time-defined supply voltage and $E(t) = \Omega_{ref} - \Omega_2$ is the previously defined error.

4.3.1

Mathematical simplifications for the closed-loop control

For mathematical simplification, some assumptions discussed earlier can be used in the composed full drilling system by substituting the parameter values in Eqs. 3-12 and 3-13. In the closed-loop system, the disturbance (resistive bit torque) is $T_1 = 0$ and the torque vector $\mathbf{T} = [0]$. Moreover, the control law $U_m(t)$ is defined in Eq. 4-5. Thus, the state-space equation of the closed-loop system is defined as:

$$\mathbf{q}' = \{\mathbf{A}_1\}\mathbf{q} + \{\mathbf{A}_2\}U_m \quad (4-6)$$

$$\mathbf{y} = \{\mathbf{A}_3\}\mathbf{q} \quad (4-7)$$

where \mathbf{q} is the state vector and \mathbf{q}' is the first derivative of the state vector, $\{\mathbf{A}_1\}$ is the set parameters matrix, $\{\mathbf{A}_2\}$ the input parameter vector controlled by the scalar control law U_m , and $\{\mathbf{A}_3\}$ is the output parameter vector.

4.4

Controlling nonlinear disturbance in drilling system

In this section the TOB is assumed as a nonlinear unmeasured disturbance in the drilling system. So, to compensate the nonlinearity generated by the TOB and to evaluate the performance of the system, four different control feedback strategies will be applied, such as:

- Proportional and Integral Controller (PI)
- Proportional, Integral and Derivative Controller (PID)
- Model Predictive Controller (MPC)
- Model Predictive Controllers and Proportional, Integral and Derivative (PID + MPC)

It is important to notice that these strategies are performed to control the angular velocity by actuating in the upper system, as assumed before. As a result, the controller generates the supply voltage of the actuator system.

4.5

Stick-slip severity (SSS)

The **Stick-Slip Severity** (*SSS*) is an instability analysis performed for the four control strategies presented before based on a stability error criterion $e_c = 10\%$. In this study, the *SSS* may be presented as a 2D and 3D color map that plots the relation between *WOB* and angular velocity (RPM), exposing limits where the previous defined torsional vibration (stick-slip) becomes severe

according to a criterion. The criterion is to compare the SSS value with the error e_c .

The 2D and 3D color maps illustrate the gravity level of the torsional vibration in a color diagram. The methodology used to construct these colored maps varies with a set of WOB (using the previously defined friction model) for a constant angular velocity, so that the same process is repeated for a set of angular velocities (RPM).

The Eq. 4-8 evaluates the instability criterion based on the difference between maximum and minimum downhole measured angular velocity (Ω_1) divided by the reference angular velocity (Ω_{ref}). Then, the map is generated iteratively by comparing the value of SSS with WOB and RPM . The determined criterion quantifies the response amplitude of the system while oscillating around the reference velocity, then classify high amplitudes in the stick-slip regime.

$$SSS = \begin{cases} \left(\frac{\Omega_1^{max} - \Omega_1^{min}}{2\Omega_{ref}} \right) \cdot 100 & \text{if } SSS \geq e_c \end{cases} \quad (4-8)$$

where Ω_1^{max} and Ω_1^{min} are respectively the maximum and minimum angular velocity of the drill bit. Ω_{ref} is the reference angular velocity.

As a result of SSS for the four control strategies, Fig. 4.6 illustrates a comparison between them all.

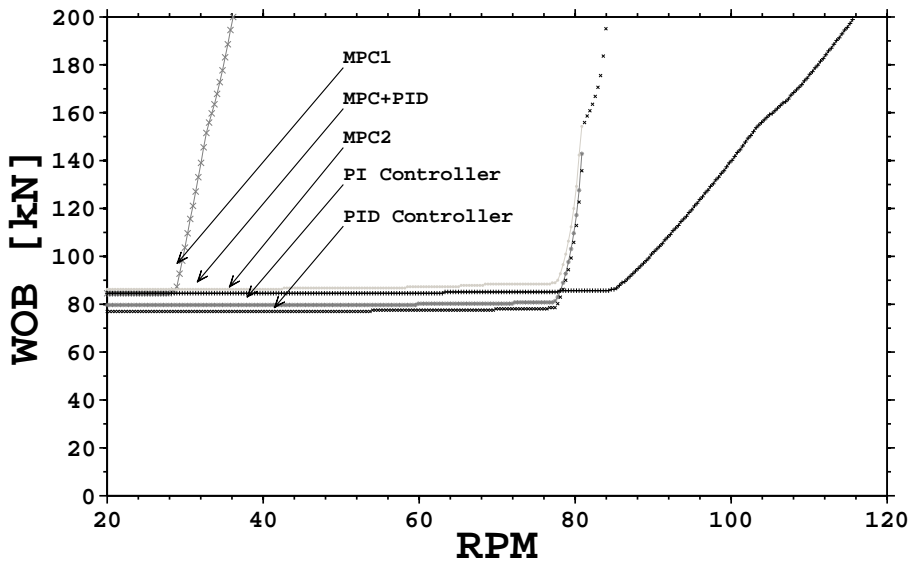


Figure 4.6: Stick-slip severity curves for the four control strategies.

5 Analysis of the results

5.1 Introduction

In this section, the results of the computational simulation of different controllers are depicted for the suppression of the stick-slip oscillations in the drilling system.

First, a structured sequence of the undisturbed open-loop system will be performed to calculate the time domain results of two subsystems. Then, numerical simulations assuming certain parameters will be performed to generate step response results of four control strategies. Finally, comparison analysis are driven to the proposed controllers.

5.2 Simulation results of the open-loop systems

The systematic procedure to evaluate the effectiveness of the open-loop analysis in control design is presented in the flowchart schematic, in Fig. 5.1. This procedure considers the defined subsystems, as modeled in Section 4.2.1. For this propose, certain physical parameters, summarized in Tab. 5.1, are assumed for both open-loop subsystems.

The open-loop analysis simulates the dynamical behavior of the subsystems (without disturbances) by varying a wide range of inputs previously defined. This approach consists, primarily, in performing a range of input torques in the drill string subsystem to achieve a range of angular velocities, similarly to those used in real applications. Then, this correlated range of angular velocities are used in the DC motor simulations to achieve the motor torque by optimizing the input supply voltage. The motor torques must be the same previously set as inputs in the drill string system.

The open-loop simulations are performed in a MATLAB code by using *Simulink* block diagrams and by regarding the iterative method presented in Fig. 5.1. The transient response of these simulations may characterize the dynamics through the following performance indicators:

1. **Rise time** – (τ_r) Time to first reach the steady-state value.

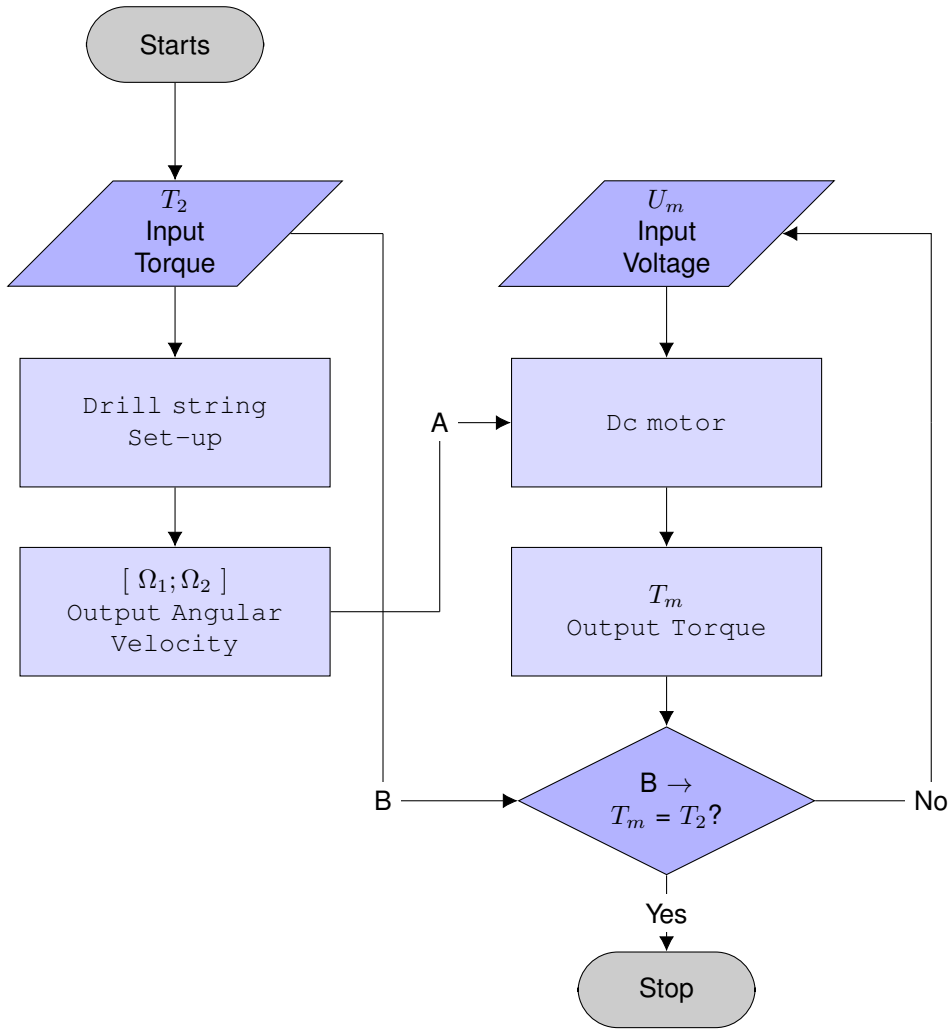


Figure 5.1: The iterative open-loop flowchart used in the analysis.

2. **Settling time**¹ – (τ_s) Time to reach and remain above the steady-state value.
3. **Peak**² – First maximum value reached by y .
4. **Peak time** – (τ_p) Time at which this peak is reached.
5. **Overshoot** – (% OS) Percentage overshoot (relative to y_{final}).

The input torque range applied in the drill string *Simulink* model varies from $2 \text{ kN} \cdot \text{m}$ to $20 \text{ kN} \cdot \text{m}$. These values were chosen based on real observation of necessary torque to achieve certain angular velocities in drilling operations.

After substituting the parameters of Tab. 5.1 into the Eq. 4-2, a summary of the open-loop surface and downhole angular velocity responses of the drill

¹Usually, the lower and upper thresholds used in the rise time calculation are 0.05 and 0.95.

²Settling Maximum

Parameter	Description	Value	Unit
ρ_{dp}	Drill string mass density	7850	kg/m^3
L_{dp}	Drill string length	4780	m
OD_{dp}	Drill string outer diameter	139.7 (5.5 in)	mm
ID_{dp}	Drill string inner diameter	118.6 (4.67 in)	mm
ρ_{bha}	BHA mass density	7850	kg/m^3
L_{bha}	BHA length	220	m
OD_{bha}	BHA outer diameter	209.55 (8.25 in)	mm
ID_{bha}	BHA inner diameter	71.40 (2.81 in)	mm
J_1	BHA + 1/3 Drill string inertia ³	322.5	$kg\ m^2$
J_2	top drive effective inertia ⁴	500	$kg\ m^2$
C_1	BHA damping	417	Nms/rad
C_2	top drive damping	50	Nms/rad
k	Drill string stiffness	521.70	Nm/rad
R	Electrical resistance	0.01	Ohm
L	Electrical inductance	0.005	H
k_e	Electromotive force constant	6	$V/rad/s$
k_t	Motor torque constant	6	Nm/Amp

Table 5.1: Simulation parameters values.

string and the DC motor systems, given in respect to time when the torque varies, are displayed in Tab. 5.2. Moreover, for each constant torque from $2\ kN \cdot m$ to $20\ kN \cdot m$ and the associated results, it is defined a Number (Num.) varying from 1 to 10, respectively, in the first column of the Tab. 5.2.

The results in Tab. 5.2 show in the last column (from left to right) the optimal voltage required by the DC motor to achieve the suggested motor torque. They also illustrated the velocity reached by the upper and lower part of the drill string when a certain torque is applied at surface. In practical terms, we may say that the system is “off bottom” due to the absence of the resistive torque disturbance. The overshoot in the upper and lower part of the system is due its natural dynamic configurations.

Multiple step responses $[\Omega_2, \Omega_1]$ of the drill string system are shown in Figs. 5.2 and 5.2. Remember that in the open-loop analysis there is no need to satisfy any control criteria or to make consistent conclusions about steady state errors, because there is no pre-defined setpoint velocity.

From the step response results, it can be seen that the system exhibits a

³Drill string proportional inertia demonstrated in [25]

⁴Top drive inertia taken from [11]

Num.	T_m^{input}	Drill string			DC Motor
		$[\Omega_1 \ \& \ \Omega_2]^{settled}$	Ω_1^{max}	Ω_2^{max}	U_m
1	$2kN \cdot m$	26.45 rpm	30.40 rpm	32.38 rpm	19.9 V
2	$4kN \cdot m$	52.91 rpm	60.80 rpm	64.76 rpm	39.9 V
3	$6kN \cdot m$	79.36 rpm	91.21 rpm	97.14 rpm	59.9 V
4	$8kN \cdot m$	105.81 rpm	121.61 rpm	129.51 rpm	79.8 V
5	$10kN \cdot m$	132.26 rpm	152.01 rpm	161.89 rpm	99.8 V
6	$12kN \cdot m$	158.71 rpm	182.41 rpm	194.27 rpm	119.7 V
7	$14kN \cdot m$	185.17 rpm	212.81 rpm	226.65 rpm	139.7 V
8	$16kN \cdot m$	211.62 rpm	243.22 rpm	259.03 rpm	159.6 V
9	$18kN \cdot m$	238.07 rpm	273.62 rpm	291.41 rpm	179.6 V
10	$20kN \cdot m$	264.52 rpm	304.02 rpm	323.79 rpm	199.5 V

Table 5.2: Drill string and DC Motor open-loop results.

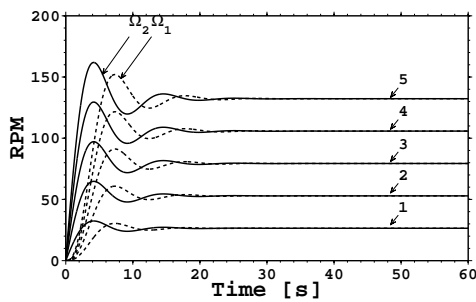
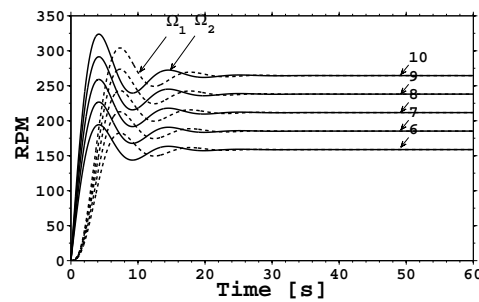
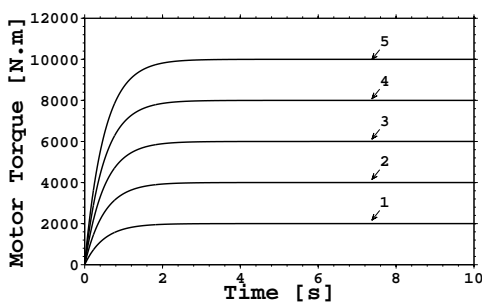
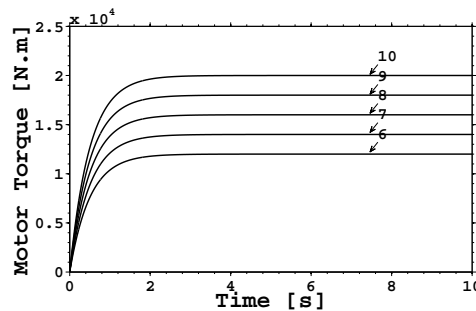
5.2(a): ($2kN \cdot m - 10kN \cdot m$)5.2(b): ($12kN \cdot m - 20kN \cdot m$)5.2(c): ($2kN \cdot m - 10kN \cdot m$)5.2(d): ($12kN \cdot m - 20kN \cdot m$)

Figure 5.2: Angular velocity and torque responses

characteristic behavior for the surface and downhole results. It becomes clearer when we analyze the performance indicators, such as rise time, establishment time, peak time and overshoot percentage. These quantities are displayed in Tab. 5.3.

These attributes show that the open-loop drill string system is completely characterized by the set of assumed parameters, since these attribute values are repeated in the 10 cases studied.

Attributes	Ω_1	Ω_2
Rise time $[\tau_r(s)]$	3.89	2.09
Settling time $[\tau_s(s)]$	14.75	16.00
Peak time $[\tau_p(s)]$	7.33	4.17
Overshoot [% OS]	14.93	22.40

Table 5.3: Attributes of the drill string step responses.

Here, the physical parameters in Tab. 5.1 and the calculated surface angular velocity (Ω_2) are used to solve the DC motor Eqs. 4-3 and 4-4. As a result, the motor torque step responses are illustrated in Figs. 5.2 and 5.2.

Figs. 5.2 and 5.2 also show that the DC motor does not present response overshoots and it has a fast response. These is more clear when we analyze the performance indicators, displayed in Tab. 5.4.

Attributes	T_m
Rise time $[\tau_r(s)]$	1.47
Settling time $[\tau_s(s)]$	1.96
Peak time $[\tau_p(s)]$	10
Overshoot [% OS]	0

Table 5.4: Attributes of the DC motor step responses.

These attributes show that the open-loop DC motor system is also completely characterized by the set of assumed parameters. Again, the attribute values are repeated in the 10 cases. Therefore, the DC motor responses are considered softer than the drill string responses and the overshoot criterion is completely satisfied.

There are many differences between the DC motor and the drill string open-loop response. For example, the overshoot percentages illustrate a great contrast in their dynamics. However, the rise time criterion resembles as it is not satisfied in both cases. The fact is that the drill string model is described more detail than the DC motor model.

Finally, even with respect to open-loop analysis, the dynamic behavior of the drill string is displayed in a *SSS* curve. The nonlinear torque disturbance is assumed in a non-controlled system, as shown in Fig. 5.3.

The *SSS* color maps (Fig. 5.3) clearly show that the transition between the non-oscillating region (in blue) and the oscillating region (in red) is extremely abrupt. Cayres [52] described different types of stability criteria, such as Lyapunov's theory, which may explain this nonlinear phenomenon.

In practical terms, if the system is operating at constant motor torque without any type of control and suffers the nonlinear perturbation caused by

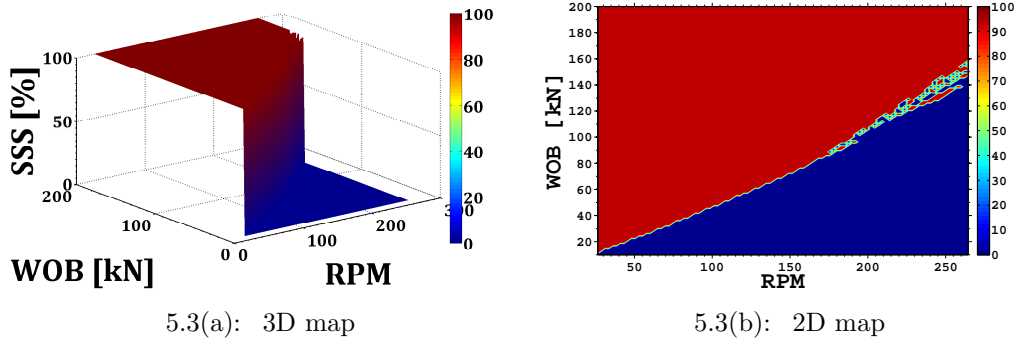


Figure 5.3: Stick-slip severity curve for open-loop system without control.

the bit-rock interaction, there are certain combinations of the pair [WOB,RPM] for which the resistive torque is greater than the constant input torque.

5.3 Simulation results of the closed-loop system without disturbance

After designing the first closed-loop system, the effectiveness of the strategy can be evaluated through the open-loop system. Therefore, the undisturbed system, presented in the block diagram in Fig. 4.5, performs simulations using the physical parameters in Tab. 5.1. A trial and error method is used to tune the control parameters in Tab. 5.5.

Parameter	Description	Value
k_p	Proportional gain	68.56
k_i	Integral gain	71.77
k_d	Derivative gain	15.13

Table 5.5: PID controller parameters tuned.

The PID controller defined in this study uses the established angular velocity of Tab. 5.2 as the reference value. Accordingly, Figs. 5.3 and 5.3 illustrate time domain results of the compensated system.

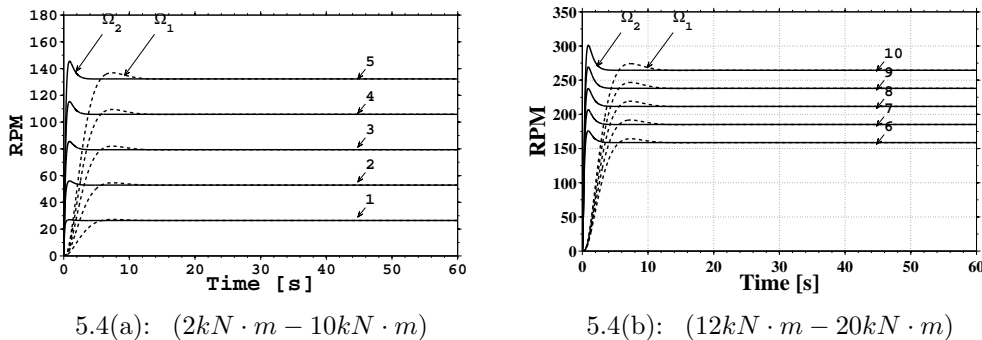


Figure 5.4: Angular velocity responses for PID controller.

By comparing the results in Figs. 5.3 and 5.3 with the open-loop results in Figs. 5.2 and 5.2 improvements can be, provisionally, perceived graphically. For example, it may be noted that the system stability, the damped behavior, and the overall velocity of the system responses improve. Performance indicators displays these quantities in Tab. 5.6.

Attributes	Ω_1^{1st}	Ω_2^{1st}	Ω_1^{5th}	Ω_2^{5th}	Ω_1^{10th}	Ω_2^{10th}
Rise time $[\tau_r(s)]$	4.34	0.29	4.15	0.39	4.06	0.40
Settling time $[\tau_s(s)]$	9.37	1.09	9.45	2.25	9.49	2.51
Peak time $[\tau_p(s)]$	7.57	0.86	7.41	0.89	7.31	0.92
Overshoot [% OS]	3.12	2.29	3.47	10.01	3.67	13.84

Table 5.6: Attributes of the drill string step responses.

The attributes of drill string step responses in a closed-loop system have a different behavior when compared to open-loop attributes. At this point, it is more difficult to characterize the system under control, due to the nonlinear environment that is inserted. For example, the rise time and the peak time decrease while the settling time and the overshoot percentage increase as the angular velocity increases. This is also probably due to nonlinearity of the system and a reflection of PID control actions.

Num.	Drill string		
	$[\Omega_1 \ \& \ \Omega_2]^{settled}$	Ω_1^{max}	Ω_2^{max}
1	26.45 rpm	27.28 rpm	27.06 rpm
2	52.90 rpm	54.64 rpm	56.03 rpm
3	79.36 rpm	82.03 rpm	85.54 rpm
4	105.81 rpm	109.43 rpm	115.38 rpm
5	132.26 rpm	136.86 rpm	145.51 rpm
6	158.71 rpm	164.29 rpm	175.92 rpm
7	185.17 rpm	191.74 rpm	206.65 rpm
8	211.62 rpm	219.22 rpm	237.73 rpm
9	238.07 rpm	246.71 rpm	269.22 rpm
10	264.52 rpm	274.23 rpm	301.13 rpm

Table 5.7: Drill-string and Closed-loop simulation performance.

The simulation information presented in Tab. 5.7 shows how the drilling system under control may improve its performance for certain parameters. In the presented system the maximum value of the Ω_2 is grater than the maximum value of the Ω_1 . However, the time settling time in Ω_1 is grater than in Ω_2 . This is the characteristics for the chosen control parameters. The settled angular velocities are the constant after the settling time.

5.4

Simulation results of the closed-loop system with disturbance

The previous section presented the performance of an undisturbed system to evaluate the effectiveness of the adopted methodology. This section, however, focuses on the behavior of the closed-loop system with nonlinear TOB disturbance. The closed-loop block diagram, shown in Fig. 4.1, will lead to the simulations for the set of control strategies mentioned in Chapter 1.

5.4.1

Proportional and integral controller (PI)

The first strategy adopted in this study is the conventional linear speed control (PI). The analysis performed in this section intends to understand the performances of the system when a set of operational procedures are applied. It is important to advise that this controller may not be sufficient to mitigate the nonlinear behavior of the system, due to its linear characteristic. However, the following simulations are intended to investigate if the controller is able to maintain the speed around a setpoint.

Parameter	Description	Value
k_p	Proportional gain	9
k_i	Integral gain	2

Table 5.8: PI controller parameters tuned.

Based on the system parameters of Tab. 5.1 and the block diagram of Fig. 4.1 a it Simulink model was designed to simulate the drill string dynamics with a feedback controller and an motor actuator. Then, using Eq. 4-8, the 2D and 3D stability color maps (*SSS*) are calculated for the drilling system submitted to a PI controller, as seen in Fig. 5.4.1.

In general, the *SSS* color maps provide two major regions to discern if the system is stable or not, as seen in Fig. 5.4.1. In addition, it is important to analyze the transition region where the dynamics becomes severe (according to the criterion adopted).

For example, it can be asserted from the color map in Fig. 5.5(a) that the angular velocity around 80 rpm represents a transition section between the oscillating and non-oscillating regions. A supercritical Hopf bifurcation diagram shows that the amplitude of vibration increases as *WOB* increases, as shown in Fig. 5.5(c).

Fig. 5.5(c) shows two bifurcation points. The first is around $WOB = 80$ kN and the most severe, around $WOB = 160$ kN. Among them there is

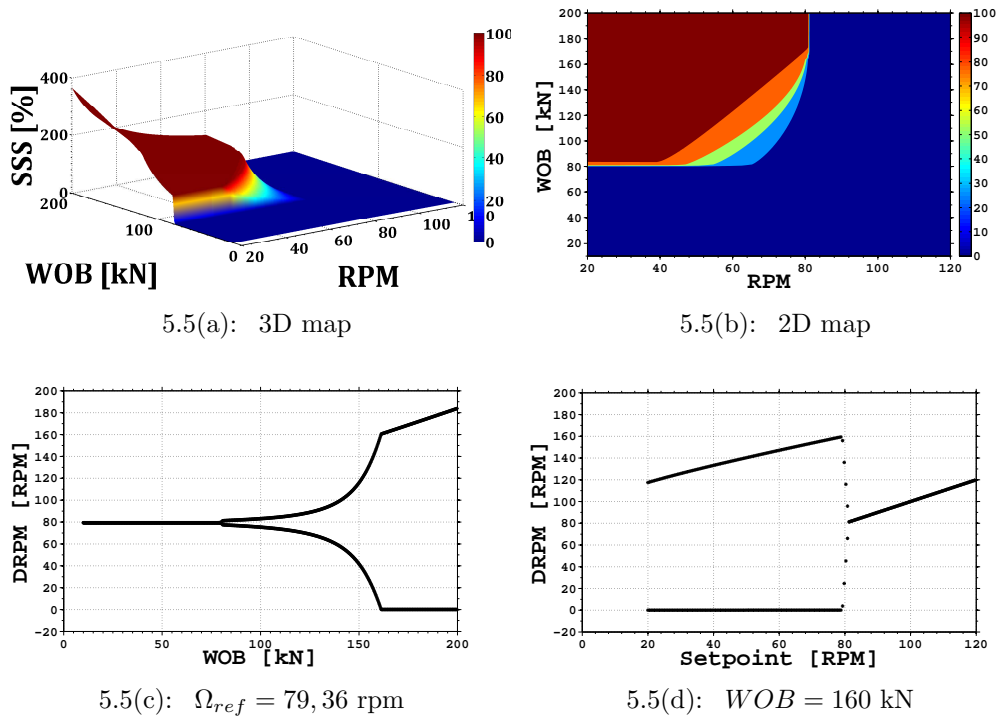


Figure 5.5: Calculated SSS and Bifurcation diagrams for PI controller.

a transition region where the oscillation increases smoothly without stopping the angular velocity. Then, after $WOB = 160$ kN, the system experiences the most severe stick-slip vibration. This behavior leads the system to a complete movement standstill and amplitudes approximately 2 times larger than the set speed (80 rpm).

Further investigations on the dynamic behavior of the downhole system set a constant $WOB = 160$ kN and vary the setpoint velocities to generate the second bifurcation diagram. This diagram compares downhole and setpoint angular velocities, as seen in Fig. 5.5(d). It may be noted that it is difficult to control the system under the established conditions. Controllability is reestablished when the speed reaches 80 rpm.

Additional numerical simulations are performed, using the PI controller, for setpoint angular velocity and WOB ranges. It is a numerical and intuitive study methodology performed for two specific situations:

- **Non-Saturated top drive rotary system** - the top drive has no torque limitation provided.
- **Saturated top drive rotary system** - the top drive has a defined profile that limits torque provided.

The following simulations evaluate the impact of torque supplied by the top drive when angular velocity varies. These results are used to generate practical recommendations for the drilling operation.

Basically, a set of angular velocities and *WOBs* are applied with the intention of attenuating the torsional vibration of the drilling operation in combination with the PI controller, as presented in Tab. The procedures use step or ramp functions to achieve four *WOBs* (30, 60, 90 and 120 kN). In parallel, step or ramp functions attempt to achieve three angular velocities (20, 60 and 100 rpm).

		Cases				
		1	2	3	4	5
<i>RPM</i>	step-zero ⁵	step	ramp	ramp	ramp + overshoot ⁶	
<i>WOB</i>	step-zero	step-zero	step-zero	ramp-zero	ramp-zero	

Table 5.9: Cases of transition functions.

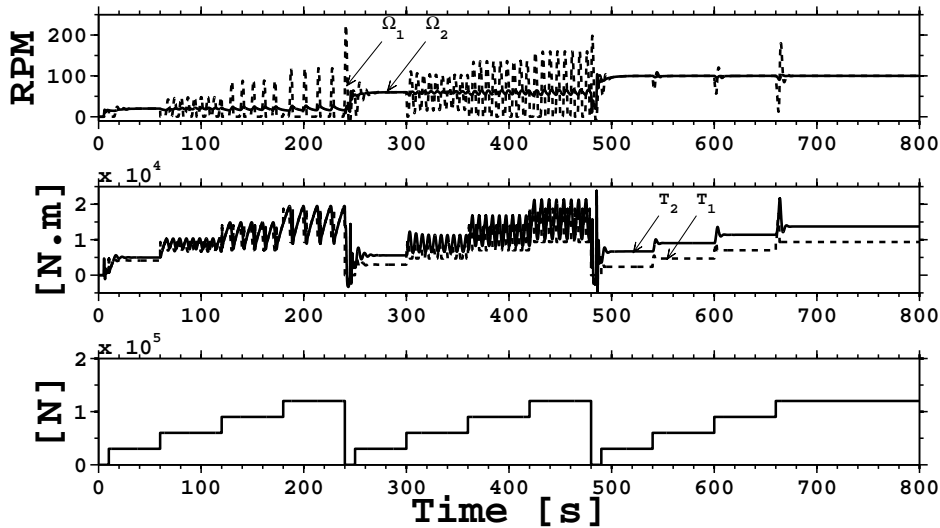


Figure 5.6: Closed-loop simulation of a top drive system (Case 1).

The donwhole angular velocity, shown in Fig. 5.6, becomes negative at $T = 240$ s (it means that the drill string tends to rotate back). This happens possibly because of the abrupt change in the *WOB* values and the angular velocity when both go to zero. In addition, the oscillation starts at $T = 60$ s with angular velocity of $\Omega_{ref} = 20$ rpm and *WOB* = 60 kN. The surface results show that the vibration is not as severe as in the downhole system.

Case 2, shown in Fig. 5.7, shows that the angular velocity does not reach zero as in the previous case, so the system response becomes softer than before. Moreover, the drill string does not rotate back at this time, although the stick-slip oscillations.

⁵Value goes to zero before reaches a new value.

⁶It is applied an overshoot on the profile.

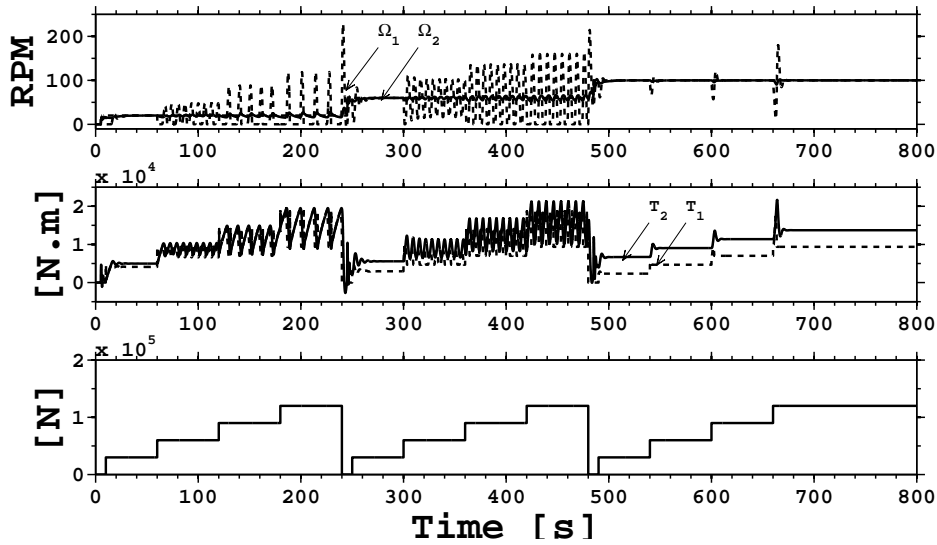


Figure 5.7: Closed-loop simulation of a top drive system (Case 2).

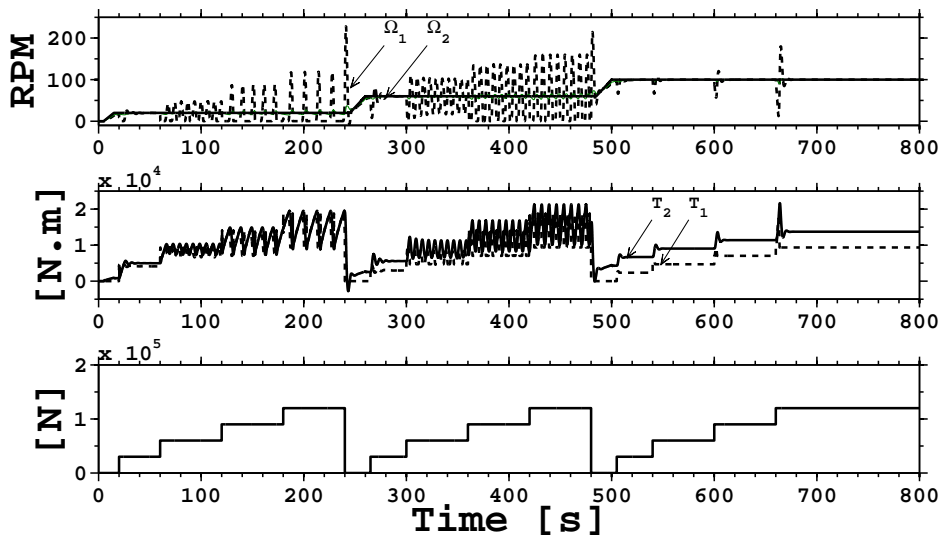


Figure 5.8: Closed-loop simulation of a top drive system (Case 3).

A ramp function is applied to rise the angular velocities in Fig. 5.8. The angular velocity and torque responses present smooth improvements in performance when compared with the last two plots.

Figs. 5.9 and 5.10 also use the non-saturated top drive. In this case, a ramp is applied to rise the WOB values. In addition, ramps provide smoother peak values of $STOR$ (T_m) in the transition. Therefore, the main difference between the two velocity values is that an overshoot is applied in the case, illustrated in Fig. 5.10, at $T = 95$ s.

The overshoot value applied in Fig. 5.10 is intended to apply additional energy to recover the stability of the system. However, this action does not

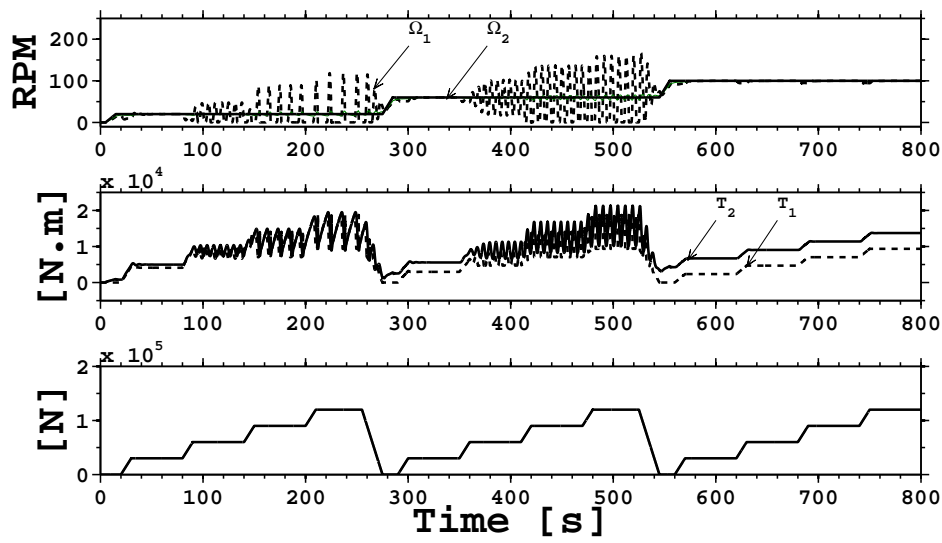


Figure 5.9: Closed-loop simulation of a top drive system (Case 4).

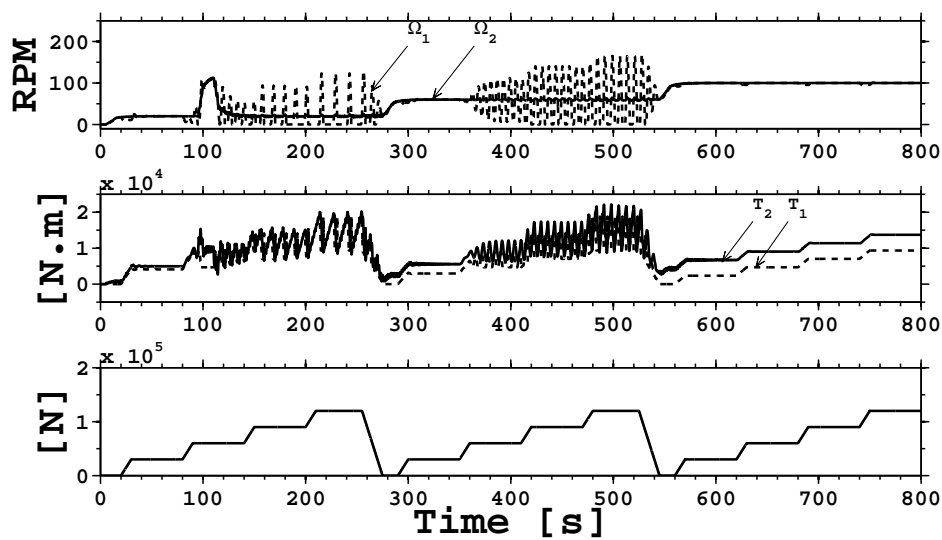


Figure 5.10: Closed-loop simulation of a top drive system (Case 5).

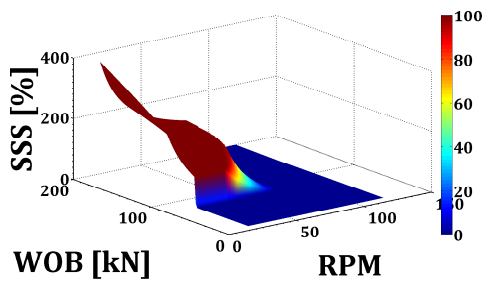
reflect the effectiveness or the controllability of this system.

5.4.2

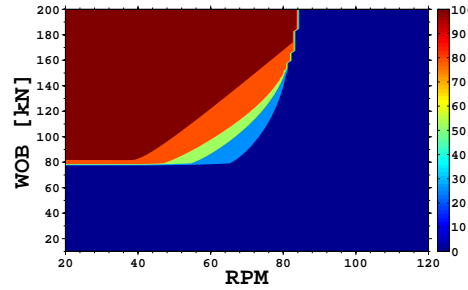
Proportional, integral and derivative controller (PID)

In this section, the linear PID controller is designed to improve the PI response. However, it still does not mitigate completely the stick-pahse for a grater range due to the nonlinearity characteristic of the problem. But the controller has established a significant improvement to the drilling system angular response.

Simulink models the PID based on the parameters of Tab. 5.1 and Tab. 5.5 and in the block diagram of Fig. 4.1. Then, the *SSS* of the system with a PID controller is calculated as the first step to characterize this control strategy, as shown in Fig. 5.4.2.



5.11(a): 3D map



5.11(b): 2D map

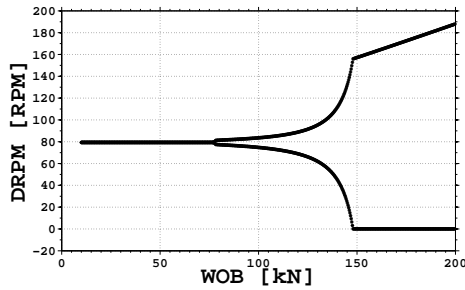
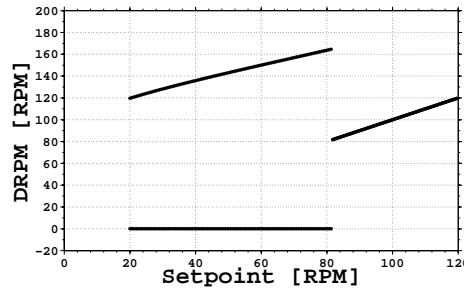
5.11(c): $\Omega_{ref} = 79,36$ rpm5.11(d): $WOB = 160$ kN

Figure 5.11: Calculated *SSS* and Bifurcation diagrams for PID controller.

The results in Fig 5.4.2 show that the stability transition region is abruptly different when compared to the open-loop *SSS* color map for the chosen criteria. However, if compared to the PI controller *SSS* curve the difference is smooth.

Similarly to the PI *SSS* color map, the angular velocity around 80-90 rpm also represents a transition region where the oscillation become more severe. A Hopf supercritical bifurcation diagram may show the amplitude of vibration increasing when different *WOB* are applied to the current system. Here, angular velocity of 80 rpm is adopted for future comparison with the previous simulation. The results are illustrated in Fig. 5.11(c).

Fig. 5.11(c) shows two bifurcation points that represent points where the oscillatory behavior begins or becomes more severe. The first is around $WOB = 80$ kN and the most severe, starts around $WOB = 150$ kN.

It may be noted from these results that PID controller will smoothly lose operating window when compared to the PI controller.

Next, a constant $WOB = 160$ kN is chosen for further investigations on the dynamic behavior of the downhole system, for a setpoint velocity range. The bifurcation diagram compares downhole and setpoint angular velocities, as seen in Fig. 5.11(d).

It can be concluded that the gain of the derivative term does not strongly affect the system when compared to the PI controller. Consequently, the system is oscillating with peaks that are slightly larger than that shown in the previous section (under the same conditions).

Thus, it is assumed the $WOB = 80$ kN acts under the conditions of the friction torque modeling (Eq. 3-14) to simulate the nonlinearity bit-rock interactions.

Although the configuration of the PID parameters has not been made correctly for a nonlinear system, the parameters in the Tab. 5.5 are still being used in these simulations. Thus, the numerical calculation is performed using the angular velocities range of Tab. 5.2, as reference input signals. The time domain results of the nonlinear system submitted to a linear compensator are shown in Fig. 5.12.

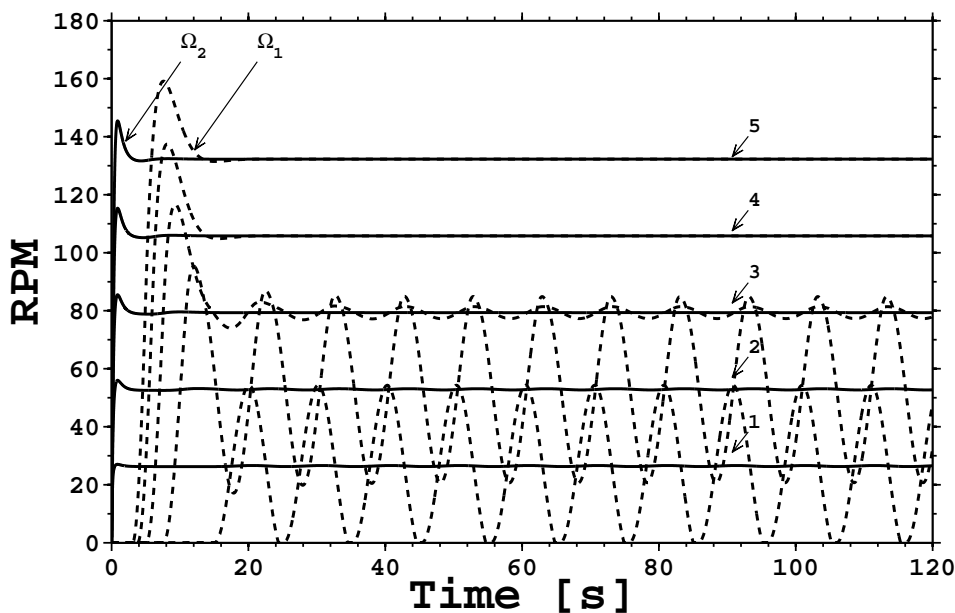


Figure 5.12: Nonlinear angular velocity responses for PID controller.

The stick-slip phenomenon may happen at low velocity and high WOB .

Based on the simulations illustrated in Fig. 5.12 the system attributes are displayed in Tab. 5.10.

Att.	Ω_1^{1st}	Ω_2^{1st}	Ω_1^{2nd}	Ω_2^{2nd}	Ω_1^{3rd}	Ω_2^{3rd}	Ω_1^{4th}	Ω_2^{4th}	Ω_1^{5th}	Ω_2^{5th}
$\tau_r(s)$	2.36	0.30	1.23	0.36	1.88	0.38	1.95	0.39	2.10	0.39
$\tau_s(s)$	N/A	1.06	N/A	1.93	N/A	2.01	12.91	2.11	12.05	2.19
$\tau_p(s)$	N/A	0.85	12.03	0.88	9.31	0.89	8.14	0.89	7.59	0.89
% OS	51.40	2.24	280.05	6.31	50.49	7.79	29.91	9.03	20.34	9.99

Table 5.10: Attributes of the drill string step responses with PID.

Thus, the attributes show that in the first three cases (1,2,3) there is no settling time in the downhole Ω_1 (the values are represented by N/A [Not Applied]). Fig. 5.12 shows that for these three setpoints there is a non-controlled oscillation that disturbs the system. However, if an angular velocity $\Omega_{ref} > 80\text{rpm}$ is applied to the system, it begins to exhibit a less severe behavior, or at least no oscillation.

A more detailed analysis is applied to the velocity of 26,45 rpm (the most severe case presented). The analysis shows the angular velocity behave on the surface and in the drill-bit, the TOB and STOR, and the supply voltage supplied by the PID controller, as seen in Fig. 5.13.

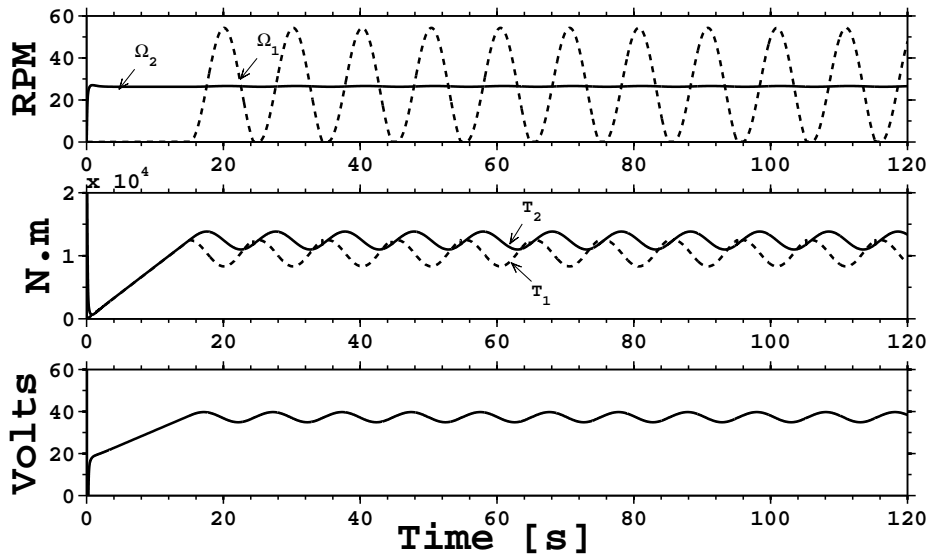


Figure 5.13: Nonlinear response of a PID Closed-loop system.

A comparison of the actual PID controller with the previous results (undisturbed PID controller system in Figs. 5.3) shows a loss of quality performance when the PID compensator is used in a nonlinear environment. An unstable angular velocity response, an undamped system, and a slow velocity response are observed, as seen in Fig. 5.13.

Tab. 5.11 summarize the simulation performance responses. For example, the maximum peak of the downhole angular velocity Ω_1 increases from an overshoot of 2.9% to a maximum of 51.3% of the reference value. However, there is no steady state error and quick response when the controller is able to mitigate the vibration. This confirms that the PID controller improves the linear part of control system.

Num.	Drill string			
	Ω_{ref}	$[\Omega_1 \ \& \ \Omega_2]^{settled}$	Ω_1^{max}	Ω_2^{max}
1	26.45 rpm	N/A	54.31 rpm	27.05 rpm
2	52.90 rpm	N/A	95.33 rpm	56.03 rpm
3	79.36 rpm	N/A	116.63 rpm	85.53 rpm
4	105.81 rpm	105.81 rpm	137.46 rpm	115.36 rpm
5	132.26 rpm	132.26 rpm	159.16 rpm	145.48 rpm

Table 5.11: Drill string with PID simulation performance.

5.4.3 Model predictive controller (MPC)

In this section, MPC is the control strategy used specifically to control the nonlinear behavior of the system. For this reason, the MPC really intends to mitigate the stick-slip phenomenon regarding the model complexity in the drilling system.

As usual, the system parameters from Tab. 5.1 and the block diagram of Fig. 4.1 are considered. In addition, a *Simulink* modeling is proposed. Thus, the system color map *SSS* when subjected to the MPC is illustrated in Fig. 5.4.3.

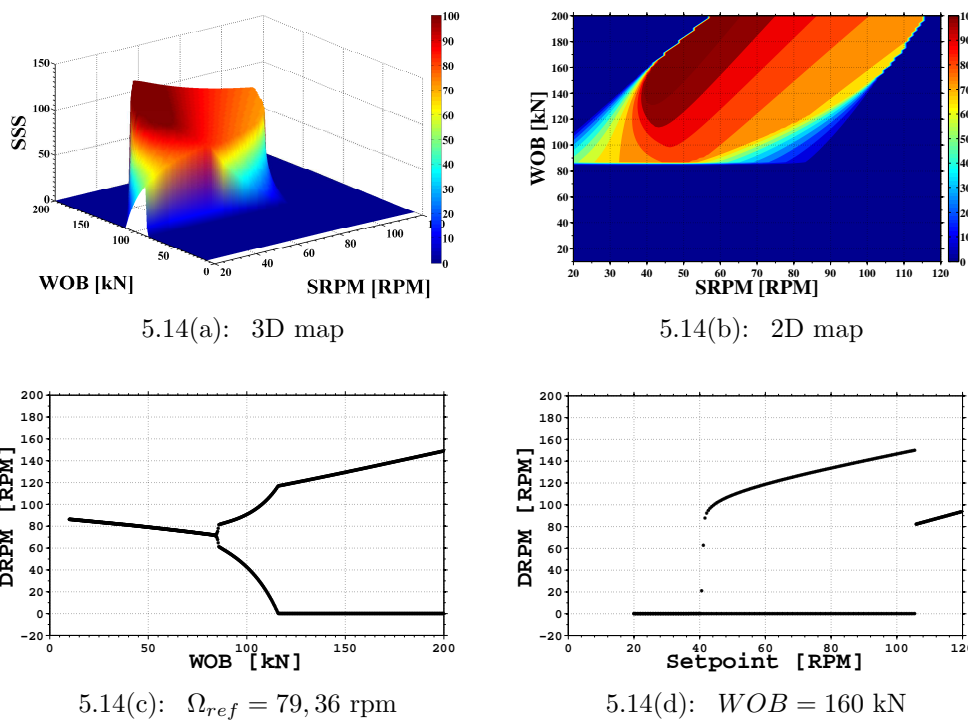


Figure 5.14: Calculated SSS and Bifurcation diagrams for MPC controller.

The *SSS* color maps of the MPC drilling system show a totally new behavior related to the stick-slip phenomenon. However, it is sensitive to the criteria adopted, as seen in Fig. 5.4.3. In practice, the MPC controls the stick-phase for the cases performed, but maintains the oscillations of steady state with low amplitude in certain.

Further analyses indicated that the blue region corresponding to *WOB* between 100 kN and 200 kN and at an angular reference speed between 20 rpm and 50 rpm is the completely stopped angular velocity (in fact, velocities are very close to zero).

The color map diagram shows a larger transition region when compared to the previous two controllers. Therefore, among several angular velocity

values in the transition region the $\Omega_{ref} = 80$ rpm is a good option for later comparison with previous cases

A Hopf supercritical bifurcation diagram may show the amplitude of vibration increasing when different *WOB* are applied to the system with MPC controller, as illustrated in Fig. 5.14(c).

Fig. 5.14(c) shows two bifurcation points. The first is around *WOB* = 85 kN. The most severe starts around *WOB* = 115 kN. It may be noted from this diagram that, as the *WOB* increases, the downhole velocity decreases. This means that this controller does not maintain the speed at the desired value but close to it.

Further investigation on the dynamic behavior of the downhole system, at constant *WOB* = 160 kN and varying the setpoint velocity, generates another bifurcation diagram. This diagram compares downhole angular velocity and setpoint angular velocity, as seen in Fig. 5.14(d).

Fig. 5.14(d) shows that at low velocity (from 20 rpm to 40 rpm) the downhole angular velocity is zero. Then, oscillations start and increase in the system until an angular velocity faster than 100 rpm. This behavior may change as a different *WOB* value is chosen.

Simulations using MPC are performed for a system with nonlinearities. For this, specific parameters were tuned using commercial software it Simulink. Then, the numerical calculations are performed using the settled angular velocity of Tab. 5.2, as reference input signal, and system parameters from Tab. 5.1. The time domain results of the nonlinear compensated system are presented in Fig. 5.15.

The system attributes, displayed in Tab. 5.12, are based on the simulations performed in Fig. 5.15.

Att.	Ω_1^{1st}	Ω_2^{1st}	Ω_1^{2nd}	Ω_2^{2nd}	Ω_1^{3rd}	Ω_2^{3rd}	Ω_1^{4th}	Ω_2^{4th}	Ω_1^{5th}	Ω_2^{5th}
$\tau_r(s)$	2.20	0.54	2.37	16.64	2.50	23.27	2.59	19.34	2.98	19.52
$\tau_s(s)$	N/A	N/A	117.39	59.42	85.47	33.26	28.37	26.11	28.51	26.22
$\tau_p(s)$	21.24	1.56	16.10	28.57	13.41	36.86	11.99	87.85	90.26	87.85
%OS	68.22	79.49	54.89	4.40	29.09	1.06	10.65	0.002	8.96e-4	0.002

Table 5.12: Attributes of the drill string step responses with MPC.

Thus, the attributes show that in the first two cases (1 and 2) there is no settling time in the downhole Ω_1 . Fig. 5.15 shows that for these setpoints there are non-controlled oscillations that disturb the system. However, if the angular velocity $\Omega_{ref} > 80$ rpm is applied in the system, it begins to run without oscillation, or at least it exhibits less severe vibrational behavior.

By choosing the most critical velocity of the results in Fig. 5.15 a more effective study can be applied to the pre-determined reference velocity

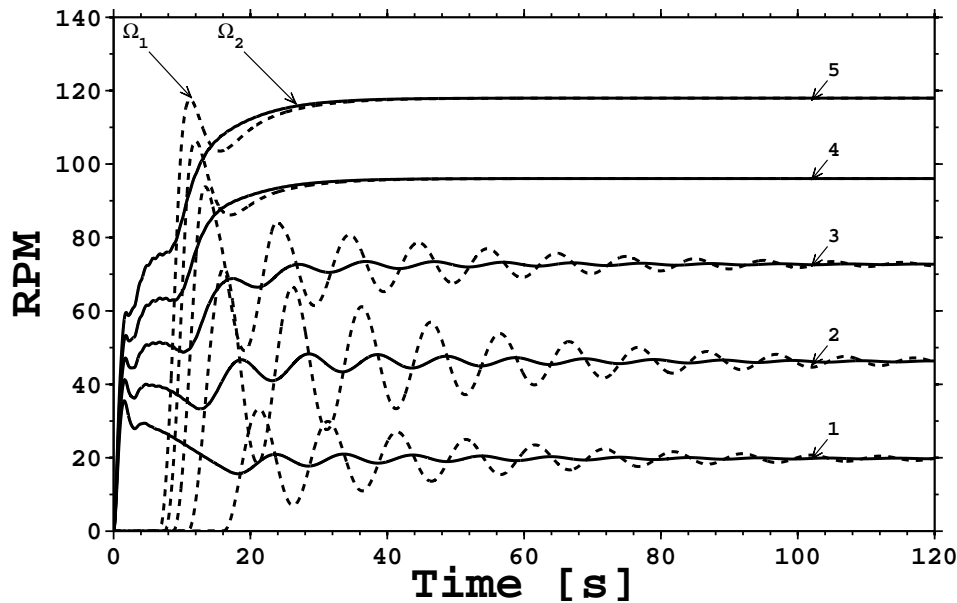


Figure 5.15: Nonlinear angular velocity responses for MPC.

26,45 rpm. Thus, the analysis consists in investigating the behavior of the angular velocity of the surface and the downhole, the TOB and the STOR, and the supply voltage, delivered by the MPC, as seen in Fig. 5.16.

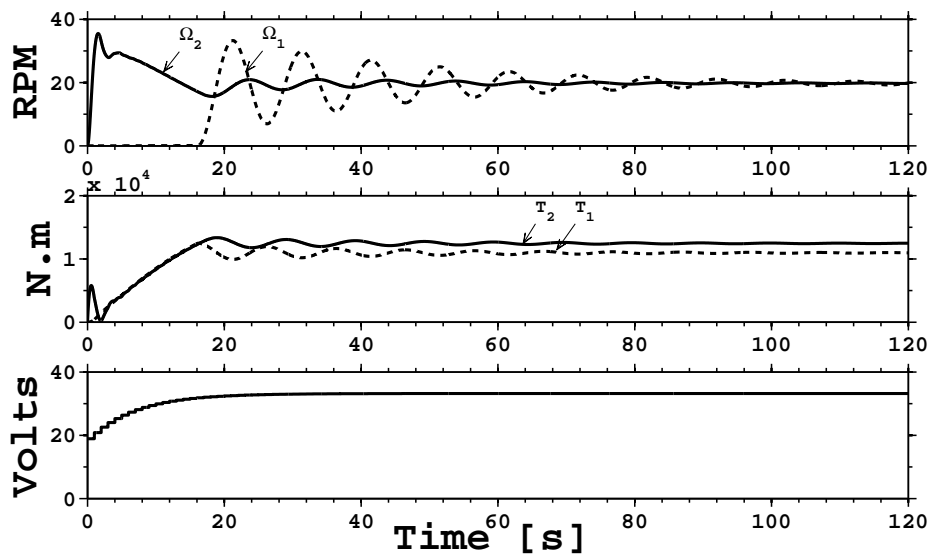


Figure 5.16: Nonlinear response of a MPC Closed-loop system.

Current MPC responses in the time domain are compared to the PID response in the undisturbed system (see Fig. 5.3). Thus, a long transient phase until the system is stable means that the speed response becomes slow when MPC is applied. The overshoot of the downhole angular velocity Ω_1 increases from 2.9% to 25% of the nominal value. Furthermore, there is a steady state

error of about 25% of the nominal value for each setpoint velocity applied.

Num.	Drill string			
	Ω_{ref}	$[\Omega_1 \ \& \ \Omega_2]^{settled}$	Ω_1^{max}	Ω_2^{max}
1	26.45 rpm	19.79 rpm	33.29 rpm	35.52 rpm
2	52.90 rpm	46.26 rpm	71.62 rpm	48.29 rpm
3	79.36 rpm	72.68 rpm	93.82 rpm	73.47 rpm
4	105.81 rpm	96.06 rpm	106.30 rpm	96.07 rpm
5	132.26 rpm	117.98 rpm	117.98 rpm	117.98 rpm

Table 5.13: Drill string with MPC simulation performance.

5.4.4 MPC and PID controllers (MPC+PID)

Designed to improve the behavior of the MPC (alone), this combined control strategy (MPC+PID) is used not only to control the nonlinearity of the system, but also to correct the equilibrium error observed in the last system. Thus, this strategy mitigates the stick-slip phenomenon under some conditions. In fact, it improves the characteristics of the drilling system by defining a better operating window.

All the simulations are based on system parameters from Tab. 5.1 and the block diagram of Fig. 4.1. A *Simulink* modeling is designed to simulate the dynamic drilling system with a motor actuator. The torsional vibration map of the drill string system when subjected to MPC+PID is illustrated in Fig. 5.4.4.

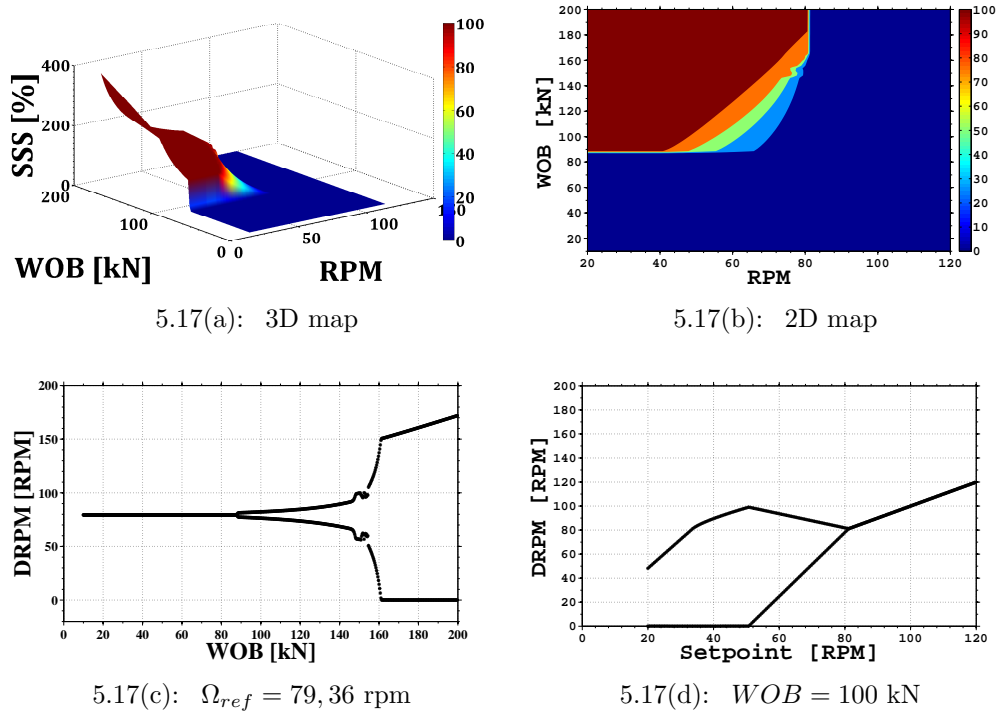


Figure 5.17:

In this case, also, it is possible to say that the angular velocity around 80 rpm represents a transition region where the oscillation has become more severe. A Hopf supercritical bifurcation diagram can show the amplitude of vibration increasing when different *WOB* are applied to the system with MPC+PID controller, as illustrated in Fig. 5.17(c).

In Fig. 5.17(c) two points of bifurcation are observed. The first is around $WOB = 90$ kN and the most severe is around $WOB = 160$ kN. However, investigations are proposed on the dynamic behavior of the downhole system

for the constant $WOB = 100$ kN and a setpoint velocity range. Therefore, the bifurcation diagram that compares the donwhole angular velocity and setpoint angular velocity is created, as seen in Fig. 5.17(d).

The general behavior of the nonlinear drilling system, illustrated in Fig. 5.4.4, evaluates the effectiveness of the combined MPC+PID control in the system. Furthermore, simulations are performed for a system with nonlinearity and some parameters are tuned to use in the MPC block diagram. The numerical calculations are performed using the range of angular velocity of Tab. 5.2, as reference input signal. The time domain results of the combined nonlinear compensator (MPC+PID) are shown in Fig. 5.18.

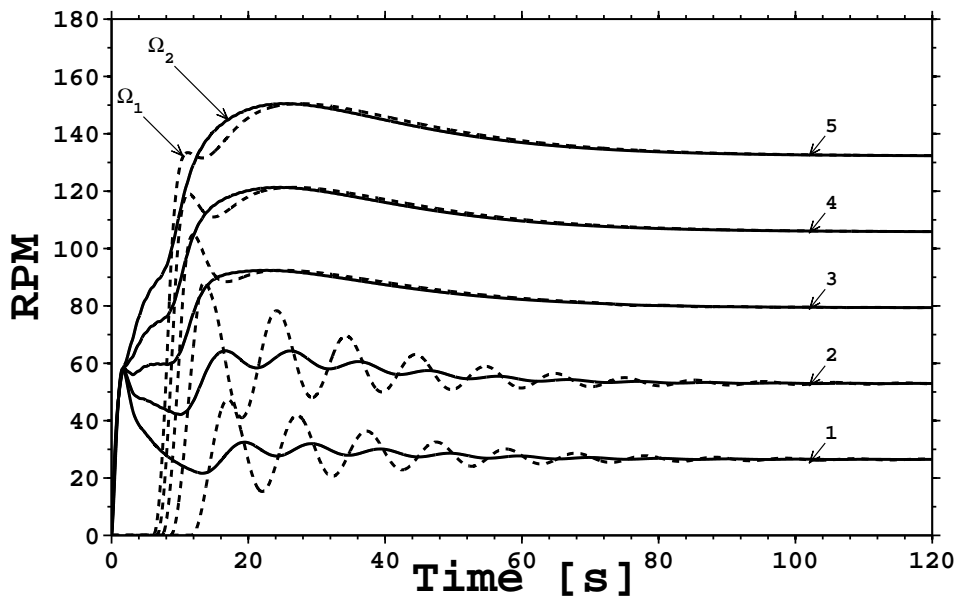


Figure 5.18: Nonlinear angular velocity responses for MPC+PID controller.

Att.	Ω_1^{1st}	Ω_2^{1st}	Ω_1^{2nd}	Ω_2^{2nd}	Ω_1^{3rd}	Ω_2^{3rd}	Ω_1^{4th}	Ω_2^{4th}	Ω_1^{5th}	Ω_2^{5th}
τ_r (s)	2.17	0.49	2.21	1.02	2.29	11.56	2.48	11.29	3.03	11.32
τ_s (s)	89.73	70.96	86.25	68.97	71.85	70.36	72.53	70.14	72.43	70.04
τ_p (s)	17.04	1.65	13.59	16.68	11.96	22.71	26.72	24.71	27.66	25.69
%OS	79.05	120.13	66.77	21.70	32.11	16.48	14.67	14.70	13.80	13.84

Table 5.14: Attributes of the drill string step responses with MPC+PID.

A specific analysis, using the critical results of Fig. 5.12, is performed to generate stick-slip phenomenon for low velocity and high WOB . Thus, studies are done for setpoint velocity of 26, 45 rpm. The analysis consists of investigating the behavior of the angular velocity at the surface and the drill-bit, the TOB and the STOR, and supply voltage delivered by the controller, as seen in Fig. 5.19.

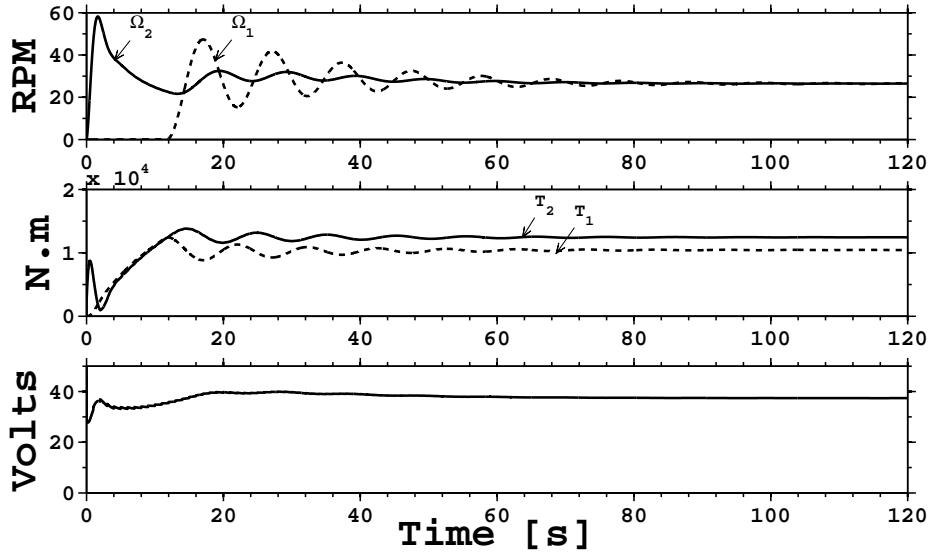


Figure 5.19: Nonlinear response of a MPC+PID Closed-loop system.

The time domain responses of the combined MPC+PID control are compared to the response of the nonlinear MPC and of the linear PID controllers, separately. In addition, the current controller is compared to the undisturbed PID controller, seen in Fig. 5.3.

Thus, MPC+PID performance enhancements show that the PID component (of the combined system) is responsible for a long transient phase until the system has stabilized and the MPC component is responsible for compensating system nonlinearity. For this reason, both systems should be tuned with different parameters than those used in previous sections. The first overshoot of the downhole angular velocity Ω_1 are between 15% to 25% of the nominal value. Furthermore, there is no steady state error of the nominal value for the chosen setpoint velocities.

Num.	Ω_{ref}	Drill string		
		$[\Omega_1 \text{ \& } \Omega_2]^{settled}$	Ω_1^{max}	Ω_2^{max}
1	26.45 rpm	26.45 rpm	47.37 rpm	58.23 rpm
2	52.90 rpm	52.90 rpm	88.23 rpm	64.38 rpm
3	79.36 rpm	79.36 rpm	104.84 rpm	92.43 rpm
4	105.81 rpm	105.81 rpm	121.33 rpm	121.37 rpm
5	132.26 rpm	132.26 rpm	150.52 rpm	150.57 rpm

Table 5.15: Drill string with MPC + PID simulation performance.

6

General conclusions and future works

6.1

Conclusions

Recalling that in the current industry overview presented in Section 1.1, the major interest of the drilling industry is to improve operational performance and reduce overall operating costs. Among several approaches in that order, the reduction or elimination of stick-slip vibration is an important step in that direction.

Note that in the literature (see Section 2.2) it is possible to find numerous studies related to stick-slip and control topics. However, when looking at the industry, there is not an ultimate model or methodology used in a practical way. Therefore, it is not an overestimation of this study to attempt to initiate such an approach.

Taking the last paragraph in mind, the author stated that the main objective of this dissertation is to minimize the problem of torsional vibration of the drill bit using existing control strategies. Also, he considers evaluation and confronting the performance of the strategies.

The main objective is subdivided into five research objectives. First, the development of an open-loop analysis of the drilling system considering a saturated and a non-saturated top drive actuator; second, the application of existing control strategies using different torque/velocity inputs in a closed-loop system; third, it is considered the control of the torsional vibration with nonlinearity due to friction interaction with the wall and in the donwhole system; fourth, it intends to evaluate a non-stop control system while drilling, fifth, it intends to implement the improvements of the model in an experimental reduced setup for future verification and validation of the models.

The main contributions of this dissertation addressing these objectives can be summarized in terms of contributions on the development of an open-loop methodology to decouple the actuator and the plant, on the application of a wide range of inputs to optimize the output of the controller (supply voltage), on controlling the stick-slip with nonlinearity due to friction in the downhole system, on the evaluation of the controller performances during

drilling operation.

- *The development of an open-loop methodology to decouple the actuator and the plant:* One of the great contributions of this study is part of the control design methodology proposed in Chapter 4. Opening the loop of the closed-loop system, with motor actuator and drill string, proved to be extremely useful in understanding the behavior of the system. The response of the open-loop drill string system provided an angular velocity related to an imposed torque. With this information, it is possible to define the appropriate top drive unit for each demand. Moreover, when applying a wide range of inputs combined with the open-loop drill string responses in the open-loop DC motor, the basis to optimize the output of the controller is provided.
- *The application of a wide range of inputs to optimize the output of the controller (supply voltage):* The steps of the interactive open-loop method for analysis are presented in Chapter 5. The results of the Section 5.2 showed the open-loop response to the imposed inputs and the optimized supply voltage. This information is important when the signal that would be controlled has to be chosen. It is also helpful to identify which control law should be used.
- *Controlling the stick-slip with nonlinearity due to friction in the downhole system:* Initially (in Section 4.4), a linear method was used to compensate the torsional vibrations in the drilling system. The conventional PI rotary speed control method attenuated and reduced torsional vibration under certain conditions. However, if the characteristics of the system change, it is only efficient when the goal is to keep the angular velocity almost stable around a set point (as in Chapter 5). So, for the linear PI control law to be defined for the disturbance generated by the stick-slip phenomena, its parameters (proportional and integral gain) must be chosen intelligently. Tucker & Wang (2003) [11] demonstrated in their study an efficient way to choose PID parameters. It is also possible to follow an orientation for automatic speed controller tuning on paper [58]. But, as applied here, the torque response generated by nonlinearity shows that this friction torque can not be efficiently compensated only by using a linear control. A robust nonlinear controller must be applied to work in conjunction with the PI rotary speed controller.

That is why the use of a model-based control is one of the most relevant actions in this study. Although the limitations found in the adopted model and settings, it is clear the powerful tool this strategy has proven to be. It was able to confront the nonlinear behavior of the system. It also

controlled and improved other control actions for the set of settings used. Due to the limitations to properly define the parameters for this, this strategy was not able to control the nonlinearity and maintain the angular velocity by itself. But in combination with the PID controller proved to be a robust strategy.

- *The evaluation of the controller performances during drilling operation:* Some of the main contributions of this work are, first, the fact that it was done on a real-scale configuration with the top drive system as the actuator. This indicates that the hardware configuration can be constructed using these parameters as the basis.

The simulation proves that speed feedback control is needed, but not enough to cure the stick-slip. The speed controller is one way to achieve the driller's needs to keep the angular velocity as stable as possible.

The bit-torque friction model used in the initial simulation represents the observed behavior of the torsional system. Once the systems are stabilized, the oscillation generated by the stick-slip phenomenon are reduced. Thus, we can conclude that the oscillations of the system reduce their velocity amplitude while the motor speed increases.

6.2

Recommendations for future research

In this final section, recommendations for future research directions are given. First, two general recommendations for future research are presented on the control theory presented in Section 2.3.1. In this section, the basic concepts of control applied in the oil and gas industry were presented.

- *Development of new controller design strategies:* The controller design strategies proposed in this study should consider the active surface control of the drilling system considering the conventional and model-based approach.
- *Robustness analysis, verification and validation on a experimental reduced drill-string setup:* The reduced drilling string configuration has already been developed and validated for a dynamic model in the Dynamics and Vibration Laboratory of the Mechanical Engineering Department of PUC-Rio. The next steps are the implementation of existing control strategies on the test rig.
- *Development of an optimization of control parameters:* The optimization of the control parameters is essential for this project, since the parameters used in this study were reached by an error and trial methodology to

approximate the optimized supply voltage. Parameters must be optimized every time the physical system settings change.

- *Controller in real time:* It is interesting to also investigate if controllers can be used in a real-time implementation. Thus, the next step of the project is to implement the control strategy mentioned in the methodology to investigate the situations mentioned.

Afterward, a torsional stability diagram of the drilling process should be drawn to better understand which variables influence the stability of the system, and then a system with the best way to mitigate the stick-slip should be developed.

- *Apply different models of bit-rock friction:* Analyze and perform simulations considering different models of bit-rock friction. This may help to better represent the behavior of the bit-rock interaction, given by the friction model. The fact is that the different friction models can represent different situations of the bit-rock interactions or of the drill pipe-wall interaction.
- *Experimental validation of friction models:* Among these different friction models it is possible to choose which one obtains superior empirical results during the drilling process. It should be remembered that the drilling process is not a singular behavior because it could change, for example, due to the variation of the load, lubrication and roughness of the surface (nature of the rocks). Thus, it is interesting to apply the control design to the different situations that have been defined.

Based on the presented methodology other configurations of the system parameters will be applied in the drilling system to analyze its behavior when applying different controllers. Settings such as drill string length, DOF numbers, WOB, Ω_{ref} , will be changed in future studies in the next phase of the work.

Bibliography

- [1] E. M. Navarro-López, “Bit-sticking Phenomena in a Multidegree-of-freedom Controlled drill string,” in *Exploration & Production*, vol. 8 of 2, pp. 70–75, 2010.
- [2] D. E. Seborg, T. F. Edgar, and D. A. Mellichamp, **Process Dynamics and Control**. New Jersey: John Wiley and Sons, Inc., 2nd ed., 2004.
- [3] M. I. Khan, T. Yasmeen, A. Shakoor, N. B. Khan, and R. Muhammad, “2014 oil plunge: Causes and impacts on renewable energy,” in *Renewable and Sustainable Energy Reviews*, vol. 68, pp. 609–622, 2017.
- [4] Bonaire Le - Nexant, “Crude-oil’s impact on renewable energy: energy alternative or energy staple?.” Online; accessed 08-Feb, 2017. <http://www.altenergymag.com/article/2015/06/crude-oil's-impact-on-renewable-energy-energy-alternative-or-energy-staple/20384/>.
- [5] C. Handscom, S. Sharabur, and J. Woxholth, “The oil and gas organization of the future.” Online; accessed 08-Feb, 2017. <http://www.mckinsey.com/industries/oil-and-gas/our-insights/the-oil-and-gas-organization-of-the-future>.
- [6] L. Van den Steen, **Suppressing Stick-Slip-Induced drill string Oscillations: A Hyperstability Approach**. PhD thesis, University of Twente, Enschede, The Netherlands, 1997.
- [7] A. F. A. Serrarens, “ H_∞ Control as Applied to Torsional drill string Dynamics,” Master’s thesis, Eindhoven University of Technology, Eindhoven, The Netherlands, 1997.
- [8] P. Sananikone, O. Karnoshirna, and D. B. White, “A Field Method for Controlling drill string Torsional Vibrations,” in *IADC/SPE Drilling Conference, SPE-23891*, (New Orleans, Louisiana), pp. 443–452, February 1992.
- [9] F. Abdulgalil and H. Siguerdidjane, “PID Based on Sliding Mode Control for Rotary Drilling System,” in *IEEE/EUROCON The International Conference on “Computer as a Tool”*, vol. 2, (Serbia & Montenegro, Belgrade), pp. 262–265, November 2005.

- [10] A. H. Suleiman, "Modeling of Stick-Slip Drillstring Vibration in Oilwell Drilling Operation," tech. rep., Universiti Teknologi MARA (UiTM), Selangor Darul Ehsan, Malaysia, 2006.
- [11] R. W. Tucker and C. Wang, "Torsional Vibration Control and Cosserat Dynamics of a Drill-Rig Assembly," in *Meccanica*, vol. 38, pp. 143–159, 2003.
- [12] A. Yigit and A. Christoforou, "Coupled Torsional and Bending Vibrations of Drillstrings Subject to Impact with Friction," in *Journal of Sound and Vibrations*, vol. 215(1), pp. 167–181, 1998.
- [13] T. G. Ritto and R. Sampaio, "Measuring the efficiency of vertical drill-string: A vibration perspective," in *Mechanics Research Communications*, vol. 52, pp. 32–39, 2013.
- [14] F. Abdulgalil and H. Siguerdidjane, "Nonlinear Friction Compensation Design for Suppressing Stick Slip Oscillations in Oil Well drill strings," in *7th IFAC DYCOPS*, (Massachusetts, USA), July 2004.
- [15] P. C. Kriesels, W. J. G. Keultjes, P. Dumont, I. Huneidi, O. O. Owoeye, and R. A. Hartmann, "Cost Savings through an Integrated Approach to drill string Vibration Control," in *SPE/IADC Middle East Drilling Technology Conference*, SPE-57555, (Abu Dhabi, United Arab Emirates), November 1999.
- [16] G. W. Halsey, A. Kyllingstad, and A. Kylling, "Torque Feedback Used to Cure Slip-Stick Motion," in *63rd Annual Technical Conference and Exhibition of the Society of Petroleum Engineers*, (Houston, TX), pp. 277–282, October 1988.
- [17] M. B. Saldivar, S. Mondié, and J. J. Loiseau, "Reducing Stick-Slip Oscillations in Oilwell drill strings," in *6th International Conference on Electrical Engineering, Computing Science and Automatic Control*, (Toluca de Lerdo, Mexico), pp. 1–6, Jan. 2009.
- [18] M. Karkoub, M. Zribi, L. Elchaar, and L. Lamont, "Robust μ -synthesis controllers for suppressing stick-slip induced vibrations in oil well drill strings," in *Multibody System Dynamics - Springer*, vol. 23, pp. 191–207, 2010.
- [19] R. B. Jijón, C. Canudas-de-Wit, S. Niculescu, and J. Dumon, "Adaptive Observer Design under Low Data Rate Transmission with Applications to Oil Well Drill-string," in *American Control Conference*, (Baltimore, Maryland), July 2010.

- [20] G. Dong and P. Chen, "A Review of the Evaluation, Control, and Application Technologies for Drill String Vibrations and Shocks in Oil and Gas Well," in *Shock and Vibration*, vol. 2016, p. 7418635, 2016.
- [21] X. Zhu, L. Tang, and Q. Yang, "A Literature Review of Approaches for Stick-Slip Vibration Suppression in Oilwell Drillstring," in *Advances in Mechanical Engineering*, vol. 6, p. 967952, 2014.
- [22] K. Javanmardi and D. T. Gaspard, "Soft Torque Rotary System Reduces Drillstring Failures," in *Oil & Gas Journal*, vol. 90 of 41, 1992.
- [23] K. Javanmardi and D. T. Gaspard, "Application of Soft-Torque Rotary Table in Mobile Bay," in *IADC/SPE Drilling Conference, SPE-23913*, (New Orleans, Louisiana), pp. 645–650, October 1992.
- [24] R. N. Worrall, I. P. J. M. Stulemeijer, J. D. Jansen, and B. G. G. Van Walstijn, "Method and system for controlling vibrations in borehole equipment." United States Patent, No. US 5117926, June 1992.
- [25] J. D. Jansen and L. van den Steen, "Active Damping of Self-Excited Torsional Vibrations in Oil Well Drillstrings," in *Journal of Sound and Vibration*, vol. 179 of 4, pp. 647–668, 1995.
- [26] J. D. Jansen, L. van den Steen, and E. Zachariassen, "Active Damping of Torsional Drillstring Vibrations With a Hydraulic Top Drive," in *European Petroleum Conference*, (London), pp. 250–254, October 1995.
- [27] R. W. Tucker and C. Wang, "On the Effective Control of Torsional Vibrations in Drilling Systems," in *Journal of Sound and Vibration*, vol. 224, pp. 101–122, 1999.
- [28] F. Abdulgalil and H. Siguerdidjane, "Backstepping Design for Controlling Rotary Drilling System," in *IEEE Conference on Control Applications*, (Toronto, Canada), pp. 120–124, August 2005.
- [29] C. Canudas-de-Wit, J. Aracil, F. Gordillo, and F. Salas, "The Oscillations Killer: a Mechanism to Eliminate Undesired Limit Cycles in Nonlinear Systems.," tech. rep., Grenoble INP, Grenoble, France, 2005.
- [30] C. Canudas-de-Wit, M. A. Corchero, F. R. Rubio, and E. M. Navarro-López, "D-OSKIL: a New Mechanism for Suppressing Stick-Slip in Oil Well Drill Strings," in *44th IEEE Conference on Decision and Control*, (Seville, Spain), pp. 8260–8265, December 2005.
- [31] M. A. Corchero, C. Canudas-de-Wit, and F. R. Rubio, "Stability of the D-OSKIL Oscillation Suppression Mechanism for Oil Well Drill-

- strings," in *45th IEEE Conference on Decision & Control*, (San Diego, USA), pp. 1846–1851, December 2006.
- [32] C. Canudas-de-Wit, F. R. Rubio, and M. A. Corchero, "D-OSKIL: A New Mechanism for Controlling Stick-Slip Oscillations in Oil Well Drillstrings," in *IEEE Transactions on Control System Technology*, vol. 16 of 06, pp. 1177–1191, 2008.
- [33] C. Canudas-de-Wit, J. Aracil, F. Gordillo, and F. Salas, "The Oscillations Killer: a Mechanism to Eliminate Undesired Limit Cycles in a Class of Nonlinear Systems," in *International Journal of Robust and Nonlinear Control*, 2008.
- [34] E. M. Navarro-López and D. Cortés, "Sliding-mode control of a multi-DOF oilwell drillstring with stick-slip oscillations," in *The 2007 American Control Conference*, (New York City, USA), July 11-13 2007.
- [35] M. Karkoub, Y. L. Abdel-Magid, and B. Balachandran, "Drill-String Torsional Vibration Suppression Using GA Optimized Controllers," in *Journal of Canadian Petroleum Technology*, vol. 48 of 12, pp. 32–38, 2009.
- [36] Z. Qi-zhi, H. Yu-yao, L. Lin, and R. Nurzat, "Sliding Mode Control of Rotary Drilling System With Stick Slip Oscillation," in *2010 2nd International Conference on Computer Engineering and Technology*, (Chengdu, China), April 16-18 2010.
- [37] Z. Qi-zhi, H. Yu-yao, L. Lin, and R. Nurzat, "A Double Surfaces Sliding Mode Control Technique in Rotary Drilling System," in *2010 2nd International Conference on Computer Engineering and Technology*, (Chengdu, China), April 16-18 2010.
- [38] S. Fubin, S. Linxiu, L. Lin, and Z. Qizhi, "Adaptive PID Control of Rotary Drilling System with Stick Slip Oscillation," in *2010 2nd International Conference on Signal Processing Systems (ICSPS)*, (Chengdu, China), pp. 289–292, July 5-7 2010.
- [39] H. Puebla and J. Alvarez-Ramirez, "Suppression of stick-slip in drillstrings: A control approach based on modeling error compensation," in *Journal of Sound and Vibration*, vol. 310, pp. 881–901, 2008.
- [40] M. K. Johannessen and T. Myrvold, "Stick-Slip Prevention of Drill Strings Using Nonlinear Model Reduction and Nonlinear Model Predictive Control," Master's thesis, Norwegian University of Science and Technology, Trondheim, Norway, 2010.
- [41] P. Sananikone, O. Karnoshirna, and D. B. White, "A Field Method for Controlling drill string Torsional Vibrations," in *SPE Americas: Un-*

- conventional Resources Conference, SPE-158109*, (Pittsburgh, Pennsylvania), pp. 443–452, July 2012.
- [42] T. G. M. Vromen, **Control of stick-slip vibrations in drilling systems**. PhD thesis, Eindhoven University of Technology, Eindhoven, The Netherlands, 2015.
- [43] K. J. Astrom and T. Hagglund, **PID Controllers: Theory, Designing, and Tuning**. Instrument Society of America, 2nd ed., 1994.
- [44] M. A. P. L. Falb, **Optimal Control: An Introduction to the Theory and Its Applications**. New York: McGraw-Hill, Inc., 1st ed., 2004.
- [45] A. G. Mutambara, **Design and Analysis of Control Systems**. Florida: CRC Press LLC, 2nd ed., 1999.
- [46] K. Ogata, **Modern Control Engineering**. New Jersey: Prentice-Hall, Inc., 3rd ed., 1997.
- [47] J. D. Jansen, **Nonlinear Dynamics of Oilwell Drillstrings**. PhD thesis, Delf University, Delf, The Netherlands, 1993.
- [48] Electronics Tutorials, “**Open-loop System and Open-loop Control Systems**.” Online; accessed 12-Jan., 2017. <http://www.electronicstutorials.ws/systems/open-loop-system.html>.
- [49] A. Ghasemloonia, D. Rideout, and S. D. Butt, “**A review of drillstring vibration modeling and suppression methods**,” in *Journal of Petroleum Science and Engineering*, vol. 131, pp. 150–164, 2015.
- [50] Electronics Tutorials, “**Closed-loop System and Closed-loop Control Systems**.” Online; accessed 12-Jan, 2017. <http://www.electronicstutorials.ws/systems/closed-loop-system.html>.
- [51] A. Sassan and B. Halimberdi, “**Design of a Controller for Suppressing the Stick-slip Oscillations in Oil well Drillstring**,” in *Research Journal of Recent Sciences*, vol. 2(6), pp. 78–82, 2013.
- [52] B. Cayres, “**Numerical and Experimental Analysis of Nonlinear Torsional Dynamics of a Drilling System**,” Master’s thesis, Pontificia Universidade Catolica do Rio de Janeiro, Rio de Janeiro, Brazil, 2013.
- [53] C. Gernay, N. Van de Wouw, H. Nijmeijer, and R. Sepulchre, “**Nonlinear Drillstring Dynamics Analysis**,” in *Society for Industrial and Applied Mathematics Journal*, vol. 8 of 02, pp. 527–553, 2009.
- [54] C. Canudas-de-Wit, K. J. A. H. Olsson, and P. Lischinsky, “**A New Model for Control of Systems with Friction**,” in *IEEE Transactions on Automatic Control*, vol. 40 of 03, pp. 419–425, 1995.

- [55] N. Mihajlovic, A. A. van Veggel, N. van de Wouw, and H. Nijmeijer, "Analysis of Friction-Induced Limit Cycling in an Experimental Drill-String System," in *Journal of Dynamic Systems, Measurement, and Control*, vol. 126, pp. 709–720, 2004.
- [56] J. F. Brett, "The Genesis of Torsional drill string Vibrations," in *SPE/IADC Drilling Conference, SPE-21943*, (Amsterdam, The Netherland), pp. 168–174, September 1992.
- [57] E. M. Navarro-López, "Practical approach to modeling and controlling stick-slip oscillations in oilwell drill strings," in *International Conference on Control Applications*, (Taipei, Taiwan), September 2-4 2004.
- [58] A. Kyllingstad and P. J. Nessjoen, "A New Stick-Slip Prevention System," in *SPE/IADC Middle Drilling Conference and Exhibition , SPE-119660*, (Amsterdam, The Netherlands), March 2009.